

NATURAL NEURONAL VARIATION IN A COMPLEX
NEUROENDOCRINE PATHWAY

Effect of selection for photoperiod responsiveness on the density and location of mature
GnRH-releasing neurons in inhibitory and excitatory photoperiods.

A Thesis Presented to

The Faculty of the Department of Biology
The College of William and Mary in Virginia

In Partial Fulfillment

Of the Requirements for the Degree of
Master of Arts

By

Mauricio Avigdor

2004

Approval Sheet

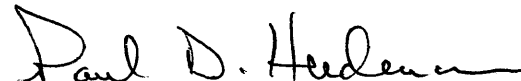
This thesis is submitted in partial fulfillment of
the requirements for the degree of

Master of Arts



Mauricio Avigdor

Approved by the Committee, April 2003



Paul D. Heideman, Chair



John D. Griffin



John P. Swaddle

Table of Contents

	Page
Acknowledgements	iv
List of Tables	v
List of Figures	vi
Abstract	vii
Introduction	2
Chapter I. Background: The GnRH neuronal system	7
Development of the GnRH neuronal system	10
Regulation of GnRH neuronal activity	11
Melatonin and the GnRH neuronal system	19
The GnRH gene	22
The GnRH peptide	23
Hypothesis and Predictions	23
Chapter II. Materials and Methods: Animals - Selected lines	27
Animals – Experiment 1	27
Animals – Experiment 2	28
Perfusions and Sectioning	29
Immunocytochemistry – Experiments 1 & 2	30
Neuron Assessment – Experiments 1 & 2	31
Experiment 3 – Relative Fiber Density	32
Statistical Analysis	34

Chapter III. Results: Experiment 1	38
Results: Experiment 2	39
Results: Experiment 3	40
Chapter IV. Discussion	62
Chapter V. Future Directions	71
Appendix	74
Bibliography	101
Vita	109

Acknowledgements

First and foremost I would like to thank Dr. Paul D. Heideman for his unending support, genuine enthusiasm, caring advice, and *nearly* infinite patience. In trying to turn me into a competent and disciplined scientist, Paul taught me how to become a more complete human being. Few people have done so much to shape my future and asked for so little in return. This thesis is as much a product of his tremendous faith in me as it is a testament of what I have learned.

Special recognition is due to the other members of my graduate committee. I am indebted to Dr. John D. Griffin and Dr. John P. Swaddle, who provided me with shining examples of intellectual excellence and discipline, as well as insight and advice throughout my research. Your generosity with access to valuable equipment and even more valuable ideas is appreciated.

My deepest gratitude goes to Dr. Emilie F. Rissman for her tremendous generosity with irreplaceable GnRH antibodies, welcoming us to her lab, allowing us to learn all the necessary techniques, and for her priceless assistance with the experimental design. Dr. Rissman's creative ideas went on to become the basis for this work.

Special thanks to the following for their assistance with this work: Jessica Tate for many days of help with perfusions and slicing, and for patiently enduring hours of non-stop club music, Dr. Diane Shakes for her kind help with image capture and processing, Michelle Rightler and the animal care staff for their help with our mice, and to Arjun Muthu for entering data. Finally, I would like to thank Justin Arocho for everything he does for me. I could write pages about it and never do him justice. Justin, your friendship and your love are so much more than anyone could ask for.

This research was supported by a grant from the National Science Foundation (9875866) to Dr. Paul D. Heideman and by the College of William and Mary.

List of Tables

Table	Page
1. Mean number of IR-neurons by major brain groups, Experiment 1	44
2. Mean number of IR-neurons by brain structure, Experiment 1	45
3. Mean number of IR-neurons by brain structure, Experiment 2	48
4. Bonferroni corrections for brain regions with P – values < 0.05	51
5. Mean number of IR-neurons by major brain groups, Experiment 2	52
6. Mean testis, seminal vesicle (SV), and body masses of RM and NRM from Experiment 2	56
7. Mean fiber density values by experimental group, Experiment 1	58
8. Mean fiber density values by experimental group, Experiment 2	59
9. Within-line effect of photoperiod on GnRH relative fiber density: RMLD and RMSD, Experiment 2	60
10. Within-line effect of photoperiod on GnRH relative fiber density: NRMLD and NRMSD, Experiment 2	61

List of Figures

Figure	Page
1. The photoneuroendocrine pathway	4
2. Mean number of GnRH neurons in RM and NRM, Experiment 1	46
3. Representative coronal sections from RM and NRM	47
4. Mean total number of GnRH neurons in RM and NRM, Experiment 2	53
5. Mean number of GnRH neurons in RM and NRM, Experiment 2, groups Rostral and Anterior	54
6. Mean number of GnRH neurons in RM and NRM, Experiment 2, groups Preoptic and Posterior	55
7. Mean number of GnRH neurons in RM and NRM, Experiment 2, group Caudal	55
8. Mean paired testis mass, SV mass, and body mass of RM and NRM, Experiment 2	56
9. ICC runs do not differ significantly: 1 factor ANOVA for 7 groups	57
10. Relative GnRH fiber density in RM and NRM, Experiment 1	58
11. Relative GnRH fiber density in RM and NRM, Experiment 2	59

Abstract

Most small mammals in the temperate zone inhibit reproduction and other non-essential functions during the winter months. Widespread individual variation in the robustness of this response has been reported, as some animals exhibit very strong reproductive regression while others show none. This study tests whether the observed variability in seasonality is related to individual differences in GnRH neuronal function, as assessed by the number and location of mature GnRH-secreting neurons and fibers.

We investigated the effect of inhibitory and excitatory photoperiods on the GnRH neuronal system of the white-footed mouse *Peromyscus leucopus*. The experiments used lines of mice previously developed by selection from a wild population, each containing largely photoperiod responsive (RM) or largely photoperiod nonresponsive individuals (NRM). Expression of mature GnRH immunoreactivity in the brain was detected using SMI-41 antibody in the single-labeled avidin-biotin-peroxidase-complex method. The location and number of mature GnRH-containing neurons were assessed in independent counts, blind with respect to treatment. Relative IR-fiber density was measured at two different brain sites. Brain regions were identified using a stereotaxic coordinate atlas for the rat brain and a stereotaxic coordinate atlas for the deer mouse (*Peromyscus maniculatus*) brain.

RM had significantly lower ($P < 0.05$) total numbers of immunoreactive GnRH neurons than NRM in short day (SD) and long day (LD) photoperiods. We detected no significant within-lines differences in the number or location of IR-GnRH cells between photoperiods. The major difference in the abundance of these neurons was found in the anterior hypothalamus and preoptic areas. RM and NRM had significantly higher relative fiber density in LD than in SD. These data suggest that changes in the amount of mature hormone secreted in LD, rather than changes in hormone synthesis, are responsible for the changes in reproductive status observed between SD and LD. Furthermore, these data suggest that individual variation in GnRH neuronal activity underlies the physiological and life history differences naturally observed in wild populations of the white-footed mouse *Peromyscus leucopus*.

NATURAL NEURONAL VARIATION IN A COMPLEX NEUROENDOCRINE PATHWAY

Effect of selection for photoperiod responsiveness on the density and location of mature GnRH-releasing neurons in inhibitory and excitatory photoperiods.

Introduction

Seasonal changes in the temperate zone lead to a temporally uneven distribution of resources needed for survival. Individuals of many species that inhabit the temperate zones limit energy expenditure during the winter months by inhibiting functions that are not essential for immediate survival, such as reproduction. This represents a useful adaptation for all endotherms, as they must cope with the increased metabolic demands imposed by the harsh, cold climate, the relative lack of available food, and the increased risk of predation associated with extended foraging time (Bronson, 1989; Bronson and Heideman, 1994).

The correct timing of the reproductive effort is of even greater importance to smaller mammals, as they are more vulnerable to the effects of harsh climate. Body size is the dominant constraining factor to an animal's physiology, morphology, and life history (Lindstedt and Swain, 1988). As body size increases, corresponding changes occur in a great number of ecologically significant characters that affect the organism's survival. Previous studies have established that traits such as gestation period, reproductive output, and time of maturation, litter size, population density, physiological time, and life span are primarily correlated to body size (Stearns, 1983; Sauer and Slade, 1988).

Small mammals tend to be short-lived, as they fall to predators at a very high rate. Their life expectancy is best measured in weeks. Most of these organisms reproduce once, if at all, and thus face enormous pressure to correctly time reproduction in order to optimize the survival of their offspring (Boyce, 1988). In order to survive, small mammals generally produce large litters of precocial offspring. Their young mature and

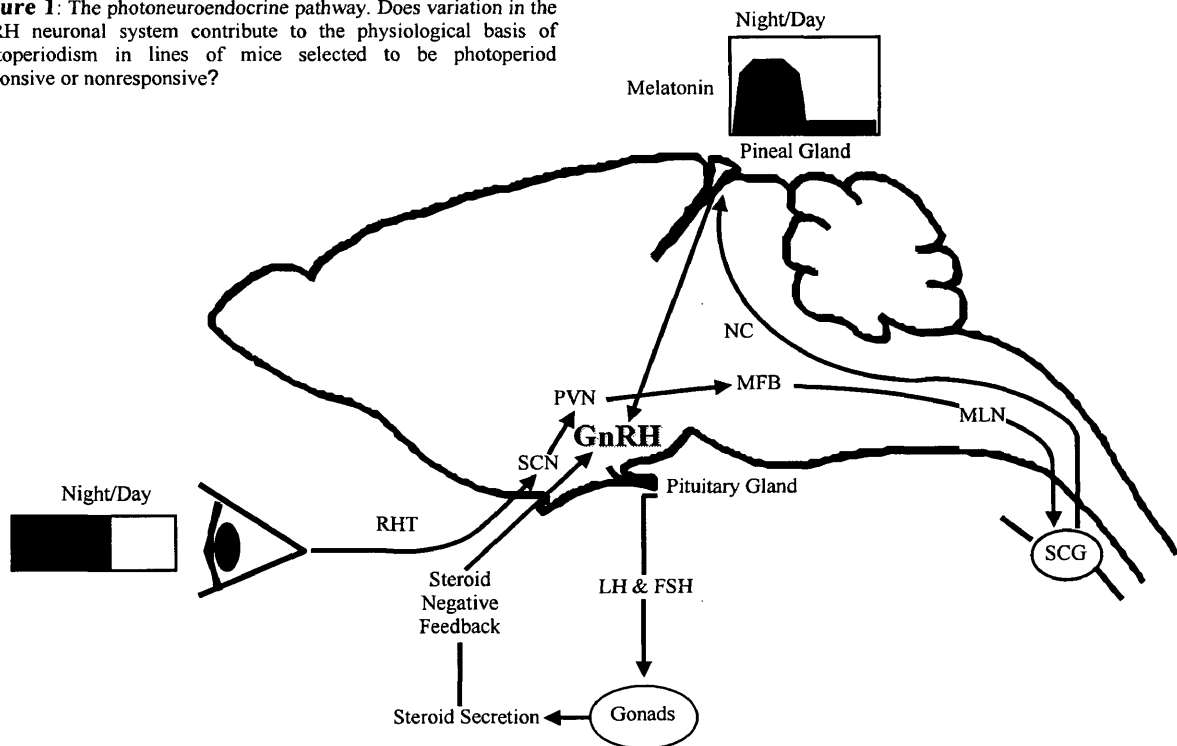
achieve sexual maturity rapidly and with significantly reduced post-natal parental care (Bronson, 1989). Small mammals, even under optimal laboratory conditions, experience a 100% to 200% increase in metabolic requirements when suckling a litter (Bronson, 1989).

Small mammals inhabiting the temperate regions rely primarily on changes in the duration of day and night in order to predict the onset of winter and regulate their reproductive status, as photoperiod is the single most reliable predictor of future conditions available to them (Bronson and Heideman, 1994). Daylength exerts effects on the mammalian reproductive system through a complex but well understood neuroendocrine pathway. The signal for light is passed from a unique class of retinal photoreceptors through the retinohypothalamic tract to the suprachiasmatic nuclei (SCN), a major component of the circadian clock necessary for timekeeping and assessment of the duration of day (Goldman, 2001). Neuronal signals are passed from the SCN to the paraventricular nuclei of the hypothalamus (PVN), to the superior cervical ganglia, and then to the pineal gland via adrenergic neurons of the sympathetic nervous system (Prendergast et al., 2002). The pineal gland releases the hormone melatonin only during the dark phase, providing a physiological signal proportional to the duration of night and day (Bartness et al., 1993; Goldman, 2001; Prendergast et al., 2002) (Figure 1).

The duration of the melatonin signal presumably alters the function of hypothalamic neurons that secrete gonadotropin releasing hormone (GnRH), a decapeptide that is the master hormonal regulator of mammalian reproduction and the final common pathway centrally controlling reproduction in vertebrates (Silverman et al., 1994; Ebling and Cronin, 2000). GnRH is released in pulses and is transported via the hypothalamic

hypophyseal portal vessels to the anterior pituitary, where it controls the release of luteinizing hormone (LH) and follicle-stimulating hormone (FSH). LH and FSH, in turn, regulate gonadal development, reproductive status, and sex-steroid production and release. Positive and negative feedback loops affect LH and FSH secretion, with testosterone from the testis inhibiting LH and FSH release, at least partially through inhibition of GnRH neurons (Bronson, 1981; Kalra and Kalra, 1983; Smith and Neill, 1987; Meredith et al., 1991; Freeman, 1994) (Figure 1).

Figure 1: The photoneuroendocrine pathway. Does variation in the GnRH neuronal system contribute to the physiological basis of photoperiodism in lines of mice selected to be photoperiod responsive or nonresponsive?



This work deals with tests of natural variation in the GnRH neuronal system and how it contributes to variation in photoresponsiveness in the white footed mouse, *Peromyscus leucopus*. Wild populations of *P. leucopus* are made up of individuals with widely different abilities to respond to photoperiod (Lynch and Gendler, 1980; Heideman and

Bronson, 1991). Some members of any given population respond strongly to the short-day photoperiod typical of the winter months by exhibiting gonadal regression or significantly delayed reproductive development. Others, the nonresponsive phenotype, seem to be capable of reproducing at all times of the year. Most individuals express an intermediate response, showing some but not all of the traits of either extreme phenotype. This suggests there is widespread, genetically based variability in the photoneuroendocrine pathway that regulates reproduction (Lynch and Gendler 1980; Heideman and Bronson, 1991; Heideman et al., 1999; Prendergast et al. 2001).

Variation in life history traits such as fertility, ontogeny, and individual responses to environmental cues is important for fitness, and also affects many ecological factors, including population dynamics. Genetic variation in life history traits may be important for rapid adaptive responses to environmental change or as a driver of population cycling. Genetic variation underlies physiological variation that leads to life history variation and the potential for life history evolution (Heideman, 2004).

While variation in life history characteristics is extremely important within and among species, almost nothing is known about the physiological variation that is responsible for life history variation in mammals. This physiological link is important because it may shape or constrain life history evolution. Because the photoneuroendocrine pathway through which environmental cues regulate winter reproduction in rodents is complex, relatively well described physiologically, and has natural populations that contain variation for the phenotype of the trait such a system, it has become a model for the study of physiological variation (Ebling and Cronin, 2000; Prendergast et al., 2002; Heideman, 2004).

Two competing hypotheses central to evolutionary physiology, the optimality hypothesis and the adequacy hypothesis, have been used in a modified form to make predictions about the extent to which complex physiological pathways are likely to be variable. Under the optimality hypothesis, a particular physiological pathway develops and is controlled by some optimal combination of the alleles present in a population (Lindstedt and Jones, 1987; Weibel et al., 1998). Optimal is defined in this context not as the optimal conceivable combination, but the optimum achievable from the alleles that already exist within a population. Under this hypothesis, natural selection should act against alleles that do not contribute to that optimum, resulting in a population holding mostly or entirely the alleles for that optimum. The consequence is that most or all individuals in a population will have a form of such a pathway that functions at the optimum level achievable. Because non-optimal alleles will be continually removed by selection, levels of variability in elements of such a pathway should be low, and the effects of any variation that is present should be neutral (Heideman, 2004). Physiologists focusing on the mechanistic aspects of complex systems often assume this hypothesis; that all components of a pathway serve an adaptive role and that the pathway itself operates optimally (see discussion in Weibel et al., 1998; Bittner and Friedman, 2000).

The major competing hypothesis is that natural selection on complex systems rarely, if ever, results in such an optimal pathway (Bartholomew, 1987; Lindstedt and Jones, 1987). Forces that counteract selection for some optimal achievable pathway may include gene interactions, including epistasis and heterosis, selective pressures that vary over time or over microgeographic location and selective pressures that differ for different physiological functions controlled by a single pathway. Under this hypothesis, natural

selection generally produces complex pathways that function only adequately, and rarely, if ever, optimally (Lindstedt and Jones, 1987; Garland, 2002; Heideman, 2004). Under the adequacy hypothesis, natural selection will act strongly only to eliminate highly deleterious alleles. Selection on most alleles may be so weak as to allow the persistence of alleles that are only slightly deleterious, on average, or alleles that can be either advantageous or deleterious, depending upon gene interactions, season, or location. A prediction from the adequacy hypothesis is that high levels of genetic and phenotypic variation should exist within complex pathways (Garland, 2002; Heideman, 2004).

Chapter 1 - Background

The GnRH neuronal system:

The mammalian GnRH neuronal complement comprises about 1000 cells, but the total number of cells making up the secretory system varies across species and appears to correlate with brain size (Wray and Hoffman-Small, 1986). Total GnRH cell numbers range from 300 to 400 in Djungarian hamsters (Yellon et al., 1990), 650 to 750 in Syrian hamsters (Jennes and Stumpf, 1980), and 500 to 1300 in the rat (Shivers et al., 1983; Wray and Hoffman-Small, 1986). The precise distribution of perykarya shows some species-specific differences. In rodents, most cell bodies are found in rostral areas such as the medial septum, diagonal band of Broca, and preoptic areas (Silverman et al., 1979; Ebling and Cronin, 2000).

The morphology of the cells themselves varies across taxa, being mostly fusiform unipolar or bipolar in rodents, and often multipolar in sheep (Lehman et al., 1986; Ebling and Cronin 2000). Ultrastructural analyses of GnRH cells reveal many morphological features that may have important functional implications. The synaptic input to GnRH neurons is very limited compared to other neurons of the preoptic area (Jennes and Conn, 1994; Silverman et al., 1994; Smith and Jennes 2001). While most neurons in the preoptic area have an estimated 6.6% of their surface area specialized for presynaptic input, GnRH neurons only have an estimated 0.4%. This corresponds to roughly five to seven synapses per GnRH perykaryon (Smith and Jennes, 2001).

In addition to the GnRH system being regulated by sparse neuronal input, studies of hypogonadal mice, an autosomal recessive mutant unable to produce GnRH, suggest

that very few neurons are required to regulate the reproductive axis (Silverman et al., 1985; Silverman et al., 1998). For example, POA grafts from wild-type mice, placed into the third ventricle of hypogonadal animals integrate with the host brain, extend to the median eminence and restore reproductive function, manifested as normal gonadal size and steroid synthesis (Silverman et al., 1985; Silverman et al., 1998). Importantly, only a small number of GnRH neurons are required to maintain reproductive function: successful grafts contained as few as three GnRH neurons. Taken together, these findings demonstrate that the GnRH system is modulated by minimal synaptic input and only requires a small number of GnRH neurons to regulate and maintain reproductive function (Kriegsfeld et al., 2002).

Thus, it is presumed that the neurotransmitters and neuropeptides that communicate with GnRH cells exert a powerful effect on their neuronal activity. Alternatively, direct presynaptic inputs to GnRH terminals at the ME could play a powerful role mediating GnRH neuronal activity, but evidence for this hypothesis is very limited (Smith and Jennes, 2001).

GnRH perykarya form several distinct subpopulations but are not segregated into nuclear clusters. Instead, they are dispersed in a loose continuum in the basal forebrain. Cells form a network that extends from the olfactory bulbs, medial septal nucleus, and triangular septal nucleus to the mediobasal hypothalamus and the retrochiasmatic zone medial to the optic tract (Silverman et al., 1994; Ebling and Cronin, 2000). Processes extend long distances and branch extensively, ending within the brain or in the capillary beds of the organum vasculosum of the lamina terminalis (OVLT) and median eminence (ME). Retrograde tracer studies in rodents indicate that 50% to 75% of all GnRH neurons

in the septal, preoptic, and hypothalamic areas are afferent to the ME, where secretion of mature hormone occurs into the pituitary portal system.

Although GnRH cells in many regions contribute to axonal bundles that project to the ME, not all cells participate in this pathway. In addition to GnRH innervation of the ME, perykarya of the septal and preoptic areas also contribute to the innervation of the OVLT, which is the second most densely GnRH-innervated structure of the central nervous system (CNS) of most species studied so far. The regulatory role of the OVLT and its associated septo-preoptico tract is unknown thus far. Treatments that lead to changes in GnRH immunoreactivity in the ME, such as castration and steroid replacement, fail to produce noticeable changes in the staining of axons of the OVLT. Due to the rapid degradation of the mature GnRH decapeptide and the existence of only a venous connection leading out of the OVLT, the target sites for GnRH released from this structure are expected to lie nearby (Smith and Jennes, 2001).

Other fibers ramify within the septum and branch throughout the septal region, with some fibers converging on the lateral ventricular wall. Fibers also appear in the subfornical organ (SFO), a structure known to possess a few GnRH neurons of its own. The fibers observed in the SFO thus have both intrinsic and extrinsic origin. GnRH neurons in the septal and preoptic regions also contribute many of the terminals found outside the hypothalamus. IR fibers extend through the stria medullaris and into the habenula. These same projections presumably innervate the pineal gland as well. Other fibers continue into the fasciculus retroflexus and terminate in the interpeduncular nucleus.

Development of the GnRH neuronal system:

GnRH neurons originate outside the CNS, in the medial olfactory placode of the midgestation embryo. In the mouse, most GnRH cells emerge from the mitotic cycle and differentiate by embryonic day 10.5 (E10.5) and commence expressing the prohormone form of GnRH a day later (Wray et al., 1989; Ebling and Cronin, 2000). By E12.5 the number of differentiated cells is similar to the number of cells that make up the adult GnRH complement, suggesting that this population gives rise to all GnRH cells in the adult animal (Silverman et al., 1994).

About half of the cells reach the nasal septum by E12.5, and briefly pause before entering the brain. This step is thought to be necessary for the establishment of a caudal pathway to the anterior hypothalamus (Fueshko et al., 1998). As they resume migration, neurons must pass through physical channels formed by the axonal fascicles of comigrating glial progenitors and their sheathing cells. Cell migration occurs from E12.5 through E16.5, from the nasal region into the medial ventral forebrain, and then into the septal, preoptic, and anterior hypothalamic areas. Axonal processes appear in the developing ME on E14.5 and are already immunoreactive to the amidated mature decapeptide. On E16.5 the GnRH neuronal network achieves its adult distribution, as cells complete the innervation of the ME. By E18 the hypophyseal-hypothalamic portal system appears in the ME and GnRH achieves the capacity to activate the pituitary-gonadal axis (Silverman et al., 1994; Ebling and Cronin 2000).

Before the olfactory area and forebrain make contact, cells expressing neural cell adhesion molecule (NCAM) migrate into the brain and form an NCAM network (Schwanzel-Fukuda et al., 1994). The vomeronasal nerve has been implicated in this

NCAM network, and pioneer axons from the nerve comigrate with GnRH neurons. While GnRH cells do not express NCAM during development and are thus unlikely to use NCAM-NCAM interactions for guidance along the fibers of the vomeronasal nerve, it seems that the NCAM network plays a permissive guiding role by creating a more attractive pathway for GnRH neuron migration (Norgren and Brackenbury, 1993).

It is believed that the neurotransmitter gamma-amino butyric acid (GABA) plays a major role mediating the brief migratory delay that GnRH cells experience during E12.5 as they progress into the CNS (Ebling and Cronin, 2000). Evidence suggests that GABA also plays a regulatory role during the migration of GnRH cells through the forebrain and anterior hypothalamus. Manipulation of the GABA_A receptor *in vivo* and *in vitro* has been shown to result in disruption in the movement of GnRH neurons out of the olfactory placode and into the brain (Fueshko et al., 1998; Bless et al., 2000; Ebling and Cronin 2000). It has not been established what other signals direct GnRH axons along their migration to the ME. Some evidence suggests that the medial basal hypothalamus releases a chemoattractive signal that leads axons into the correct direction (Rogers et al., 1997). One candidate signal is the diffusible molecule netrin. Transgenic mice with a knockout of the netrin-1 gene or the netrin receptor exhibit reduced innervation of the ME (Deiner and Sretavan, 1999). Netrin receptors have not yet been found to be expressed by GnRH neurons.

Regulation of GnRH neuronal activity:

Input to even small numbers of GnRH cells is biologically meaningful. One study of GnRH synaptic input reported one or fewer synapses per GnRH cell in the rostral

hypothalamus and POA of rats (Witkin, 1989). Axodendritic synapses were quantified in a subsequent study, with approximately four synapses per GnRH dendrite found in female rats and approximately three synapses seen on each GnRH cell body (Chen et al., 1990).

GnRH secretion is sensitive to inhibition by steroid negative feedback, but the exact nature of steroid influence on GnRH neurons is not yet understood. Until recently, it was thought that steroids modulated GnRH activity indirectly through the activation or inhibition of afferent neurons only. It is clear that inputs from afferent neurons are required for pulsatile release of GnRH, but recent experiments suggest that some GnRH neurons may contain estrogen receptors (Skynner et al., 1999; Hrabovsky et al., 2000).

Noradrenaline and adrenaline originating from neurons in the brain stem are known to play a stimulatory role in GnRH secretion. Adrenergic and noradrenergic axons are juxtaposed to GnRH neurons in the septum-diagonal band of Broca, a region in which large numbers of GnRH neurons are contained (Wright and Jennes, 1993). Immunohistochemical triple-labeling studies (Hosny and Jennes, 1998) have been used to simultaneously localize GnRH peptide, dopamine- β -hydroxylase, and α_{1B} -adrenergic receptor protein. The results show that about 80% of all GnRH neurons in the septum-diagonal band of Broca-preoptic area contain patches of IR- α_{1B} -adrenergic receptor protein at or near the plasma membrane, and that some of these adrenergic receptors are adjacent to dopamine- β -hydroxylase containing axons (Hosny and Jennes, 1998).

The GnRH neurons which did not contain α_{1B} -adrenergic receptors were preferentially located in the rostral portion of the septum and diagonal band, while all GnRH neurons in the caudal septum, diagonal band, and preoptic area expressed α_{1B} -

adrenergic receptors. Only a few α_{1B} -adrenergic receptor patches were seen in the external layer of the ME, and these receptors were rarely observed to be associated with GnRH axon terminals. This suggests that the effects of noradrenaline on GnRH release, while partly mediated by activation of α_{1B} -adrenergic receptors, is not regulated at the site of the ME (Hosny and Jennes, 1998). Since the α_{1B} -adrenergic receptor is also found in GnRH cells located away from adrenergic and noradrenergic axons, it is presumed that these catecholamines exert their effects through asynaptic release and diffusion (Smith and Jennes, 2001).

Destruction of noradrenaline neurons in the brain stem or local inhibition of α -adrenergic receptors decreases pulsatile secretion of LH as well as cyclic LH release during the estrus LH surge, possibly through disruption of GnRH secretion. Noradrenaline appears to promote or allow interactions between neurons that alter GnRH cell function. Noradrenaline also seems to play a role mediating some of the stimulatory effects of estradiol on GnRH secretion during the preovulatory period (Herbison, 1997; Smith and Jennes, 2001). Most studies on the role of adrenaline in the control of GnRH have used α -adrenergic receptor antagonists as well as inhibitors of dopamine- β -hydroxylase activity. It is possible that the observed effects on GnRH release are actually caused by adrenaline (Smith and Jennes, 2001).

5-Hydroxytryptamine (5-HT; Serotonin) is synthesized by neurons of the raphe nuclei. This neurotransmitter also plays an important role in the generation of the LH surge (Kalra 1993; Kordon et al., 1994). However, only about 5% of nerve terminal boutons adjacent to GnRH neurons are serotonergic, and in-situ hybridization studies have failed to detect any 5-HT receptor mRNA in GnRH perykarya. One hypothesis is

that 5-HT, acting through the 5-HT_{2A} receptor, exerts its effects on GnRH cells through interneurons (Wright and Jennes 1993; Smith and Jennes 2001).

Much of the regulation of GnRH neurons appears to be accomplished by local circuits. Anatomical studies have demonstrated that extensive projections to the vicinity of GnRH perykarya originate from cell bodies within the preoptic area and hypothalamus, particularly the arcuate nucleus (Simonian et al., 1999). Neurotransmission of excitatory amino acids in the brain principally involves glutamate and aspartate. L-Glutamate is the major excitatory neurotransmitter in the mammalian CNS, acting through both ligand gated ion channels and G-protein coupled receptors. The ion gated glutamate receptors are multimeric assemblies of four or five subunits, and are subdivided into three groups based on their pharmacology structural similarities: AMPA, NMDA, and Kainate receptors (Aarts and Tymianski, 2004). Excitatory amino acids induce a rapid increase in GnRH release, protein content in GnRH cells, and GnRH mRNA in their nuclei (Brann and Mahesh, 1997), whereas inhibition of glutamate receptor subunits has the opposite effect. Increased glutamate and aspartate release in the preoptic region usually precedes or parallels the estrus LH surge (Smith and Jennes, 2001).

Glutamatergic input to GnRH neurons is likely to be mediated by direct synapses at the GnRH cell bodies or dendrites, or by asynaptic neurotransmission at the ME (Kawakami et al., 1998). About half of all GnRH neurons are known to have kainic acid 2 (KA₂) receptor mRNA, and preferentially express the protein during the estrus LH surge (Eyigor and Jennes, 1996). The KA₂ subunit is a likely constituent of many neuronal kainate receptors, because it is widely expressed in most neurons in the CNS.

Multimeric assemblies of kainite receptor subunits form glutamate-gated ion channels that mediate excitatory postsynaptic currents and function as presynaptic modulators of neurotransmitter release at some central synapses (Aarts and Tymianski, 2004).

Due to the multiple possible combinations of individual subunits, many different subtypes of the N-methyl-D-aspartate (NMDA) receptor are expressed in the brain. Efficient NMDA receptor activation requires not only NMDA but also a co-agonist, glycine. Activation can also be modulated by the binding of polyamines. Recent experiments suggest that about 80% of all GnRH neurons may express the NMDAR₁ receptor subtype (Ottem and Petersen, 2000). A feedback mechanism involving estrogen receptor α protein appears to mediate the effects of estrogen on glutamate neurons, especially those of the preoptic region (Smith and Jennes, 2001).

γ -Aminobutyric acid (GABA) is the major inhibitory amino acid in the brain. A majority of the functional synaptic input demonstrated to GnRH neurons to date is GABAergic (Sim et al., 2000; Jansen et al., 2003); thus, these signals are poised to exert significant effects on GnRH neuron output. Unlike most mature neurons, GnRH neurons can be excited by GABA_A receptor activation (DeFazio et al., 2002). A significant proportion of GnRH neurons are known to express GABA_A and GABA_B receptors (Petersen et al., 1993; Jung et al., 1998). Metabolic cues from leptin, NPY, and endogenous opiates, potent regulators of both food intake and fertility, are communicated to GnRH neurons via GABAergic afferents (Smith and Jennes, 2001).

GABA is also likely to inhibit GnRH neurons directly as nerve terminals containing glutamic acid decarboxylase, the enzyme that mediates GABA synthesis, make synaptic contacts with GnRH cell bodies in the rat medial preoptic area (Smith and

Jennes, 2001). The GABAergic neuronal network in the anterior hypothalamus is also known to be sensitive to steroid-negative feedback and to play a role in the switch to positive feedback during the estrus LH surge (Wagner et al., 2001; Smith and Jennes, 2001).

Short-term fasting in mice causes rapid suppression of LH and presumably GnRH pulsatility as well (Sullivan et al. 2003), whereas refeeding rapidly reinitiates LH release (Foster et al., 1989). A recent report showed that a 48 hour fasting period decreased the frequency of postsynaptic currents GnRH neurons receive via the GABA_A receptor (Sullivan et al. 2003; Sullivan and Moenter, 2004). Interestingly, *in vivo* treatment of fasting mice with a leptin regimen known to restore fertility (Ahima et al., 1996; Sullivan et al., 2002) restored GABAergic drive to GnRH neurons to the levels seen in fed animals (Sullivan et al. 2003; Sullivan and Moenter, 2004). These data suggest that modulation of the activity of GABAergic afferents to GnRH neurons may contribute to inhibition of fertility by negative energy balance as well as fertility restoration by permissive leptin signals.

These observations indicate that metabolic signals act acutely to alter the output of the reproductive axis. The GABAergic system is poised for rapid communication with GnRH neurons. Anatomical and functional evidence suggests an interplay between hypothalamic GABAergic neurons and various metabolic peptides, including leptin (Sullivan et al., 2003; Ovesjo et al., 2001), which provides a permissive metabolic cue (Ahima et al., 1996), neuropeptide Y (NPY) (Pronchuck et al., 2002; Pu et al., 1999; Sullivan and Moenter, 2004) and opiate peptides (Cowley et al., 2001; Will et al., 2003; Sullivan and Moenter, 2004), which can act antagonistically to leptin in the regulation of

both fertility and food intake (Kalra et al., 1991; Catzeflis et al., 1993; Raposinho et al., 2001; Sullivan and Moenter 2004).

Neuropeptide Y (NPY) is a 36 aminoacid peptide whose precise role in fertility regulation in the whole animal remains unclear but appears to be state dependent (Sullivan and Moenter, 2004). In some animal models, NPY has a stimulatory effect on the reproductive axis, as it is known to facilitate GnRH release and potentiate the responsiveness of gonadotrophs to GnRH (Crowley and Kalra, 1987; Kalra, 1993; Besecke and Levine, 1994). Recent experiments demonstrate that NPY may inhibit fertility by decreasing the activity of GABAergic neurons afferent to GnRH neurons, an effect probably mediated via the NPY-1 receptor subtype (Sullivan and Moenter, 2004). This NPY effect, together with the observation that leptin rapidly increases GABAergic input to GnRH neurons, suggest a neural mechanism by which these metabolic signals may act antagonistically with one another in the regulation of fertility and possibly satiety (Sullivan and Moenter 2004).

Two distinct populations of NPY-producing cells are responsible for innervation of the hypothalamus and preoptic area. The first originates in the arcuate nucleus, where roughly 15% of all NPY neurons express estrogen receptor α . The other originates in the brain stem, where NPY neurons co-localize with noradrenaline but do not express estrogen receptors (Simonian and Herbison, 1997). NPY-containing terminals originating in both the arcuate nucleus and brain stem project to the ME and to the septum-preoptic region. Axons in the preoptic areas make synaptic contacts with GnRH cell bodies and processes, although the only evidence for neuropeptide Y1 receptors in GnRH perykarya has been found at the median eminence (Li et al., 1999).

Neurotensin, a peptide found in many neurons of the preoptic areas, is known to stimulate GnRH activity. Neurotensin neurons appear to communicate directly with GnRH neurons, a process mediated by at least three different receptors. The high affinity NT1 receptor is thought to mediate the physiological effects of neurotensin (Rostene and Alexander, 1997); the roles of nt2 and nt3 are not yet well understood. Increased expression of neurotensin in the rostral portion of the medial preoptic nucleus may directly stimulate GnRH neurons on proestrus, contributing to the LH surge. The responsiveness of GnRH neurons to neurotensin stimulation appears to be enhanced on proestrus due to increased expression of neurotensin receptors within GnRH neurons (Smith and Wise, 2001).

Endogenous opioid peptides are an important part of the inhibitory component of the neural circuitry that regulates GnRH neuronal activity and secretion (Kalra, 1993). Information about the steroidal milieu appears to be transmitted to GnRH neurons by β -endorphin acting via μ -opioid receptors. Perykarya containing β -endorphin are only found in the periarculate region of the medial basal hypothalamus. β -endorphin nerve terminals are known to synapse with perykarya and dendrites of GnRH neurons in the rat. Opioid receptor μ - and δ - mRNAs have only been found on GnRH fibers, but not on the cell bodies (Mitchell et al., 1997; Sanella and Petersen, 1997; Eckersell and Micevych, 1998). Opioid receptors are present in many other cells of the hypothalamus and preoptic area, suggesting a role for interneurons in β -endorphin inhibition of GnRH neuronal activity (Smith and Jennes, 2001).

Vasoactive intestinal polypeptide (VIP) has been identified as a critical neurochemical messenger that relays time-of-day information from the circadian

oscillator to the GnRH neuronal system, although the precise mechanisms by which the SCN transmits circadian information to GnRH neurons is not fully known (van der Beek et al., 1997). VIP is synthesized in the ventrolateral aspect of the SCN, where most of the fibers that appose with GnRH neurons originate. Approximately 40% of all GnRH cells express the VIP2 receptor protein, indicating that most of the VIP input to GnRH is direct and probably synaptic (Smith et al. 2000; Smith and Jenness, 2001). VIPergic neurons synapse in a sex differentiated manner in the medial preoptic area, with females exhibiting a greater number of contacts per neuron (van der Beek et al., 1993). GnRH neurons receiving innervation from VIP cells in the SCN are preferentially activated during the LH surge (van der Beek; et al., 1994), further suggesting a role for VIP regulation of the timing of estrus.

Melatonin and the GnRH neuronal system:

Differences in the density or affinity of the melatonin receptors that ultimately affect mature GnRH secretion are likely to play a role in the naturally-occurring variation in photoperiod responsiveness observed in most populations (Heideman et al., 1999). Various areas of the hypothalamus have been shown to express melatonin receptors, but these overlap very little with areas containing GnRH perikarya (Bittman, 1993; Heideman et al., 1999). The exact mechanism by which melatonin influences GnRH release is not yet known, but it is likely to involve the MT1 melatonin receptor. Of the three known melatonin receptor subtypes (MT1, MT2, and MT3), only MT1 and MT2 have been implicated in modulating circadian rhythms (Witt-Enderby et al., 2003). However, Siberian hamsters lacking a functional MT2 receptor exhibit seasonal

reproductive and circadian responses to melatonin, suggesting that only the MT1 receptor mediates circadian and reproductive responses to melatonin (Weaver et al., 1996).

The antagonistic action of melatonin has been thought to involve the suppression of the release of GnRH from neurons in the *P. leucopus* hypothalamus (Glass and Knotts, 1987). Short photoperiods, as well as melatonin treatment, have been shown to have a modulatory effect on GnRH secretion in hypothalamic fragments from adult rodents (Kao and Weisz, 1977). *In vitro* incubations of male rat hypothalamic tissue with melatonin suggest diurnal mechanisms by which melatonin can either facilitate or suppress GnRH release. Experiments on the GT1-7 immortal cell line of GnRH-secreting neurons indicate that the regulation of GnRH gene expression and secretion by melatonin appears to be under coordinated control by the PKA, PKC, and MAPK pathways (Roy and Belsham, 2002). The down-regulation of GnRH gene expression and secretion in GT1-7 cells by melatonin supports the hypothesis that the hypothalamus is a major target tissue for the antagonistic action of melatonin. The effects of melatonin on GT1-7 cell function appear to occur partly through G protein-coupled receptor-mediated signaling mechanisms that, in the short term, result in the inhibition of cAMP, the activation of PKC and MAPK, and the induction of the immediate early genes *c-fos* and *junB* (Roy and Belsham, 2002).

Within the rodent pituitary gland, melatonin-binding sites appear shortly after the formation of Rathke's pouch (Davis, 1997). As this region differentiates into the adenohypophysis, melatonin receptors are transiently expressed in the pars distalis during late fetal development and then disappear over the initial 2–3 weeks of postnatal life (Vanecek, 1988). In contrast, MT₁ melatonin receptors remain expressed in the pars

tuberalis into adulthood (Hazlerigg, 2001). Hence, there is developmental and tissue-specific control of melatonin receptor expression in the pituitary (Johnston et al., 2003).

In the newborn rat, the loss of pars distalis melatonin receptors occurs in parallel with a reduced ability of melatonin to inhibit GnRH-induced LH secretion from gonadotroph cells (Martin and Sattler, 1979). It has been speculated that the decreased inhibition of the pituitary-gonadal axis by melatonin may contribute to the timing of puberty in mammals (Martin and Sattler, 1979). The molecular mechanisms that determine the marked developmental and tissue-specific profiles of melatonin receptor expression have not been investigated in any tissue so far (Johnston et al., 2003).

The upstream fragment of the rat MT₁ gene is known to possess multiple response elements for the transcription factor pituitary homeobox-1 (Pitx-1), which is expressed in the anterior pituitary (Johnston et al., 2003). Johnston et al. (2003) demonstrated that a Pitx-1 expression vector could stimulate expression of both MT₁-luciferase and luteinizing hormone β -subunit (LH β)-luciferase reporter constructs in COS-7 culture cells. The transcription factor EGF-1, which is directly induced by pulsatile GnRH release and activates LH β expression, was found to attenuate Pitx-1-induced MT₁-luciferase activity (Johnston et al., 2003). In a related experiment, pituitary MT₁ gene expression was found to be 4-fold higher in hypogonadal mice, which do not synthesize GnRH, than in their wild-type littermates. These data suggest that maturation and activation of the GnRH pulse generator might be the causal factor resulting in the postnatal loss of melatonin sensitivity in gonadotrophs and pituitary MT₁ gene expression (Johnston et al., 2003).

The GnRH gene:

The gene encoding GnRH has been localized to a single locus on chromosome 8 in the human (Yang-Feng et al., 1986) and to chromosome 14 in the mouse (Williamson et al., 1991). The gene spans 4.5 kb of DNA and consists of three introns separating four small exons. GnRH-encoding regions are approximately 500 bases long and contain an open reading frame of 276 nucleotides (Bond et al., 1989; Adelman et al., 1986; Sagrillo et al., 1996). The first exon encodes a 5' untranslated region of mRNA, followed by the second exon, which encodes several domains within the GnRH precursor protein. These regions include the signal sequence, the GnRH decapeptide, the precursor processing signal, and the first 11 amino acids of gonadotropin-associated peptide (GAP), a biologically active peptide contained within the GnRH propeptide that has been implicated in the inhibition of prolactin secretion (Sagrillo et al., 1996; Nikolics et al., 1985; Yu et al., 1988). The third and fourth exons encode the remaining amino acid residues of GAP, the termination of transcription codon, and the 3' untranslated region of the message.

Regulation of transcription varies across species. In mouse and humans, transcription is initiated from a single promoter located in the 5' flanking region of the GnRH gene (Radovick et al., 1990; Yu et al., 1994). A stimulatory estrogen response element has been identified in distal regions of the human promoter, suggesting that steroids may play a role regulating GnRH gene expression (Radovick et al., 1991). Transcription in the rat seems to originate from one major and possibly two minor promoter regions (Bond et al., 1992; Kepa et al., 1992). Furthermore, the rat promoter

may contain activating and inhibitory regions that may be important for GnRH expression (Kepa et al., 1992).

The GnRH peptide:

The GnRH gene encodes a large precursor protein, preproGnRH, consisting of 92 amino acids and having a molecular weight of approximately 10,000 kDa (Sagrillo et al., 1996). The first 21 amino acids of the preprohormone form a typical signal sequence with a characteristic hydrophobic center. Two serine residues follow, and then the decapeptide sequence of GnRH. Once the signal peptide is cleaved, a single glutamic acid residue at the N-terminus of GnRH undergoes cyclization to produce pyroglutamic acid. At this point the C-terminal end of proGnRH is still linked to the remainder of the precursor, the 56-aminoacid peptide GAP. A glycine-lysine-arginine triplet between the two peptides acts as a cleavage site and signals the carboxyl-terminal amidation of GnRH to form mature peptide (Seeburg and Adelman, 1984; Sagrillo et al., 1996).

Individual variation in the GnRH neuronal complement - hypothesis and predictions:

Previous experiments conducted on an unselected colony of *P. leucopus* (Glass, 1986) and an unselected colony of *Peromyscus maniculatus* (Korytko et al., 1998) indicate that reproductively responsive males inhibited by a short-day photoperiod possess greater numbers of immunoreactive GnRH (IR-GnRH) neurons than nonresponsive males. The antibodies used in the immunocytochemistry of these studies, GnRH-BDB (Glass, 1986) and LR1-GnRH (Korytko et al., 1995; Korytko et al., 1998) are known to bind to an epitope of pro-GnRH. It has been suggested that responsive

males sequester prohormone in the neurons that synthesize GnRH, but fail to secrete mature peptide when placed in inhibitory photoperiods (Glass and Knotts, 1987; Korytko et al., 1997; Korytko et al., 1998). Thus, responsive mice are proposed to retain more prohormone than nonresponsive mice, resulting in more neurons immunoreactive to an antibody specific to an epitope of proGnRH. In these previous studies, the majority of the IR-GnRH neurons of *P. maniculatus* were found within seven regions in and around the hypothalamus. Significant differences in neuronal location and density could be traced to two of those: the lateral hypothalamus and the preoptic areas (Korytko et al., 1995, Korytko et al., 1998).

Experiment 1 tested the hypothesis that genetically based; selected line-specific differences in photoperiod responsiveness are accompanied by variation in GnRH neuron activity, as manifested by the number and location of cells producing mature GnRH neuropeptide under an inhibitory photoperiod. We proposed that *P. leucopus* belonging to a line artificially selected for strong inhibition of reproduction in short photoperiod (Responsive mice, RM) would produce and secrete lower levels of mature GnRH than animals from a line selected to be reproductively active in short photoperiod (Nonresponsive mice, NRM). Therefore we predicted that RM would exhibit significantly lower total numbers of IR-GnRH cells following processing with an antibody specific to mature GnRH, because GnRH neurons with prohormone but little or no mature GnRH would remain unlabeled. Furthermore, on the basis of results by Glass (1986) and Korytko et al. (1998), we predicted that significant differences in the number of IR-GnRH cells between selection lines (RM and NRM) would be manifest in a small

region of the brain encompassing the anterior/lateral hypothalamus and the preoptic areas.

Experiment 2 tested two hypotheses that arose from, and are consistent with the results obtained in Experiment 1. First, that NRM have higher total numbers of GnRH neurons, which results in a higher number of cells producing mature hormone in NRM than in RM at all times, and permits reproductive activity even if some suppression of GnRH secretion occurs in SD. Based on this hypothesis, we proposed that NRM in a permissive, long day photoperiod (NRMLD) might secrete higher levels of mature GnRH than RM in long day photoperiod (RMLD). Therefore we predicted that NRMLD would exhibit significantly higher total numbers of IR-GnRH cells following processing with an antibody specific to mature GnRH. Furthermore, we predicted that significant differences in the number of IR-GnRH cells between selection lines and photoperiod treatments (RMLD, RMSD, NRMLD, and NRMSD) would be manifest in a small region of the brain encompassing the anterior/lateral hypothalamus and the preoptic areas.

The alternative hypothesis is that RM and NRM have nearly identical total numbers of GnRH neurons, but line-specific variation in the proportion of GnRH cells producing and secreting mature neuropeptide in short photoperiod is responsible for the differences observed in Experiment 1. Based on this hypothesis, we proposed that RMLD would secrete levels of mature GnRH nearly identical to those secreted by NRMLD. Therefore we predicted that RMLD and NRMLD would exhibit no significant differences in the total numbers of IR-GnRH cells following processing with an antibody specific to mature GnRH, but that significant differences would be manifest between RMLD and

RMSD because GnRH neurons with prohormone but little or no mature GnRH would remain unlabeled.

Experiment 3 tested the hypothesis that genetically based differences in photoperiod responsiveness are accompanied by variation in GnRH fibers; as manifested by differences in the mean fiber content of mature GnRH neuropeptide between selected lines in an inhibitory photoperiod. We proposed that RMSD would secrete lower levels of mature GnRH than NRMSD. Therefore we predicted that RMSD would exhibit significantly lower mean relative fiber density than NRMSD because GnRH neurons with prohormone but little or no mature hormone would remain unlabeled. This experiment, along with Experiment 2, also tested the hypothesis that responsive males sequester prohormone in the neurons that synthesize GnRH, but fail to secrete mature peptide when placed in inhibitory photoperiods. We predicted that RMSD would differ significantly from RMLD in relative fiber density of mature GnRH-releasing neurons, but that NRMSD would not significantly differ from NRMLD as NRM secrete mature hormone irrespective of photoperiod conditions.

Chapter 2- Materials and Methods:

Animals – Selected lines:

Mice were obtained from a laboratory colony at the Population and Endocrinology Laboratory of The College of William and Mary. The wild founders of the population were captured in the vicinity of Williamsburg, Virginia. Wild-caught animals were paired in a long-day (LD) photoperiod (16L:8D), yielding a parental generation to serve as stock for selection experiments. To establish photoperiod-responsive and photoperiod-nonresponsive lines, animals from the parental generation were examined at 70 days of age and assigned a reproductive index based on testis size or the size of the ovaries, uterine diameter, and presence or absence of visible corpora lutea (Heideman et al. 1999). Males with a testis index $<24 \text{ mm}^2$ were classified as responsive, those with a testis index $>32 \text{ mm}^2$ were classified as nonresponsive (Heideman and Bronson 1991; Heideman et al. 1999). Responsive males and females were paired to produce a photoperiod-responsive line. Nonresponsive males and females were paired to produce a nonresponsive line (Heideman et al. 1999).

Animals - Experiment 1:

Experiment 1 was performed on young adult *P. leucopus* from the line selected to be strongly photoresponsive (RM) and the line selected to be nonresponsive (NRM). Mice in this experiment were from the F4 to F6 selected generations. Mothers and their pups were transferred from LD photoperiod to short-day (SD) photoperiod (8L:16D) within three days of birth of the litter. Male offspring were weaned at 21-23 days and

singly housed until age 70 ± 3 days of age. RM chosen for this study ($n = 8$) had a testis index $<24 \text{ mm}^2$, which is typical of suppressed males. 95% of RM males produced in the colony at the time of the study fit the selection criteria. NRM chosen for this study ($n = 9$) had a testis index $>40 \text{ mm}^2$, which is typical of reproductive males in LD. Of the NRM males produced at the time of this study, 50% fit the selection criteria.

Because GnRH secretion is sensitive to inhibition by steroid negative feedback and NRM presumably differ from RM in sex steroid secretion, we chose to control for individual differences in sex-steroid production in this experiment. Mice chosen for this study were castrated and provided with a silastic implant (1.02 mm ID, 5 mm in length) filled with evenly mixed testosterone (Sigma Chemical Co. St. Louis, MO) in silicone adhesive in a 1:3 ratio by mass. This treatment causes seminal vesicles to develop to a size typical of reproductively mature males (P.D. Heideman, unpublished data). Mice were allowed to acclimate to the hormone treatment for two weeks prior to perfusion. Food (Agway Prolab Rat/Mouse/Hamster 3000, Syracuse, NY) and water were provided ad libitum. During periods over which experiments were performed, the relative humidity of the animal rooms averaged $60\% \pm 20\%$, and the room temperature was $23^\circ\text{C} \pm 3^\circ\text{C}$.

Animals – Experiment 2:

Experiment 2 was performed on two groups of young adult *P. leucopus* from each of the two selected lines described above, resulting in four different treatment groups of animals. Mice in this experiment were from the F6 to F9 selected generations. RM and NRM raised in SD photoperiod (RMSD, $n = 14$; and NRMSD, $n = 13$) were produced by transferring mothers and their pups from LD photoperiod to SD photoperiod within three

days of birth of the litter. Male offspring were weaned at 21-23 days, singly housed until 70 ± 3 days of age when their testis index was assessed, and singly housed again until perfusion. RM and NRM in LD (RMLD, $n = 14$; and NRMLD $n = 14$) were born, raised, weaned at 21-23 days, assessed at age 70 ± 3 for their testis index, and singly housed until perfusion under a 16L:8D photoperiod. Mice were chosen at random from each of the selected lines, but no sibling pairs were included. Thus, mice whose testis index at age 70 ± 3 days did not meet the selection criteria for their line were still included in this experiment. Based on results by Korytko et al. (1997) and to compare with our own results from Experiment 1 for effects of endogenous steroids, it was decided to use intact mice that had not undergone castration and steroid replacement treatment by silastic implant. Mice from this experiment were anesthetized and weighed immediately prior to perfusion.

Perfusions and Sectioning:

All perfusions were conducted in mice aged 70-100 days. Mice were euthanized with an overdose of Isoflurane (Abbot Laboratories, North Chicago, IL) and were allowed to enter respiratory arrest prior to perfusion. Mice were perfused through the left ventricle at approximately 4 ml/min using a perfusion pump and bled via the right atrium. Perfusion of 5 ml of 0.1 M phosphate-buffered saline at a pH of 7.4 (PBS) was followed by perfusion of 50 ml of fresh, cold (5°C) 4% paraformaldehyde (Fisher Scientific, Fair Lawn, NJ) and saturated picric acid (Sigma Chemical Co. St. Louis, MO) in PBS. Brains were removed and post-fixed overnight at 4°C in 0.1 M PBS with 30% sucrose for cryoprotection. The mass of the paired seminal vesicles was assessed in animals from

Experiment 1 and Experiment 2. The mass of the paired testis was assessed in animals from Experiment 2 only. All brains were sliced within 4 days of perfusion. Frozen coronal sections (30 μ m) were cut on a freezing sliding microtome and separated into four wells, each containing every fourth section. Wells were filled with brain antifreeze (37.5% sucrose, 37.5% ethylene glycol, and 10g PVP-40 in 500 ml 0.02 M Tris-buffered saline). Brains were stored at -20°C until immunocytochemistry.

Immunocytochemistry – Experiments 1 & 2:

Expression of mature GnRH immunoreactivity in the brain was detected using a single-labeled avidin-biotin-peroxidase-complex method. A total of three independent runs were carried out in Experiment 1, and a total of seven independent ICC runs were carried out in Experiment 2. Each independent run was balanced across treatments. Brain slices were rinsed 5 times for 6 min each in cold 0.02 M Tris-buffered saline (TBS) followed by incubation in cold (4°C) 1% sodium borohydride (Sigma Chemical Co. St. Louis, MO) for 30 min. All subsequent treatments were conducted with gentle agitation at room temperature unless otherwise noted. Tissue was rinsed 3 times for 10 min each in cold TBS, followed by overnight incubation at room temperature with SMI-41 monoclonal antibody (Sternberger Monoclonals, Lutherville, MA) at a dilution of 1:20,000 in PBS with 0.25% lambda-carrageenan (Sigma Chemical Co. St. Louis, MO), 1% bovine serum albumin (BSA) (Sigma Chemical Co. St. Louis, MO), and 0.3% Triton X-100 (Fisher Scientific, Fair Lawn, NJ) in TBS with 0.1% sodium azide at a pH of 7.8 (Fisher Scientific, Fair Lawn, NJ). SMI-41 is a mouse monoclonal IgG1 antibody reactive with the five amino acids adjacent to the C-terminus of the GnRH peptide and

the amidation site. Therefore only mature hormone is likely to be recognized by SMI-41 antiserum (Tai et al. 1997). Sections were given six 10-min rinses in TBS and incubated in biotinylated horse anti-mouse IgG at a dilution of 1:500 in TBS with 0.25% lambda carrageenan, 1% BSA, and 0.3% Triton X-100 for 60 min at room temperature. After 3 more rinses in 0.02 M TBS, sections were incubated in avidin-biotin-peroxidase (Vector Laboratories Elite ABC-Peroxidase kit) in TBS for 60 min. Sections were given 3 rinses in TBS and placed in 1.5 ml of a solution of diaminobenzidine (DAB)(0.2 mg/ml), NiSO₄ (24 mg/ml), and diluted H₂O₂ (4.8 μl/ml of freshly prepared solution from 35 μl of 30% H₂O₂ in 965 μl of distilled H₂O) (Sigma Chemical Co. St. Louis, MO), in 0.02 M TBS. The color reaction was allowed to proceed for approximately 12 min. After five 10-min rinses in 0.02 M TBS, sections were mounted on gelatin-coated slides and air dried, dehydrated in xylene, and coverslipped with Permount (Fisher Scientific, Fair Lawn, NJ).

Neuron Assessment – Experiments 1 & 2:

The location and number of mature GnRH-secreting neurons in Experiment 1 were assessed in independent counts by the author of this thesis and by P.D. Heideman, carried out blind with respect to treatment using an Olympus CH2 compound light microscope. The location and number of mature GnRH-secreting neurons in Experiment 2 were assessed in a single count by the author, carried out blind with respect to treatment using the same equipment previously described.

Brain areas were first estimated relative to major landmarks using a stereotaxic coordinate atlas for the rat brain (Paxinos and Watson, 1986). The regions where IR-

GnRH cells were scored using the brain atlas for the rat were later compared to those identified in a stereotaxic coordinate atlas for the deermouse, *Peromyscus maniculatus* (Eleftheriou and Zolovick, 1965). Because the deer mouse atlas lacked detail in much of the hypothalamus, the rat brain atlas was used to estimate boundaries of many of the brain areas, and terminology from this latter source is used here. *P. leucopus* have much larger eyes and optic nerves than the similarly sized laboratory mouse, and in our judgment the hypothalamic structures and landmarks are more similar to those of the rat than those of the lab mouse.

IR-GnRH cells were found in the region limited rostrally by the horizontal limb of the diagonal band of Broca, and caudally by the arcuate hypothalamic nucleus and medial tuberal nucleus. The numbers and locations of neurons identified in independent counts by M. Avigdor and P.D. Heideman were very similar, the overall results were qualitatively identical, and both data sets gave identical statistical results. This consistency indicated that independent recounts were not necessary for the animals of Experiment 2. The data presented here are those measured by the author. All brain structures and nuclei in this paper are referred to using abbreviations and nomenclature consistent with those given by Paxinos and Watson (1986).

Experiment 3 – Relative Fiber Density:

Fiber density serves as a semi-quantitative relative measure of differences in immunoreactive material present in a sample of tissue. In this study, relative fiber density is affected by three factors: the number of IR-GnRH fibers present in any one section of tissue treated with antibody, how dark each IR-fiber is, and how much IR-GnRH is

present in the background, outside neuron fibers. A Leitz Laborlux-S light microscope with a 10X objective and a Sony XC-77 video camera module with a 0.7X coupler were used for image capture. NIH Image V. 1.62 software was used for image processing and fiber density measurements. An objective micrometer graded at 0.01 mm was used to assess the dimensions of the boxes where fiber density measurements were taken.

Measurements were taken in two different sections from each brain. Areas chosen for measurement were easy to identify due to their proximity to major brain landmarks, and contain abundant clusters of IR-fibers. One measurement was taken at the anteromedial preoptic area (AMPO), in the section of each brain that corresponds to Plate 20 of the Paxinos and Watson rat atlas (1986). Measurements were taken for all brains of Experiments 1 and 2 following the same procedure. A $50 \times 50 \pm 2$ pixel box ($\sim 95 \times 95 \mu\text{m}$) was created and a background measurement taken at the optic chiasma (ox). Microscope light intensity was adjusted in order to standardize all background grayscale values to 65 ± 3 on a 1 to 256 intensity grayscale. The box was then dragged to the AMPO to obtain a measurement of the area of interest. The background value was subtracted from the value of the area of interest to obtain a relative fiber density measurement.

The second measurement was taken at the arcuate hypothalamic nucleus (Arc), which corresponds to plates 29 through 31 of the Paxinos and Watson rat atlas (1986). In all cases the darkest of the three sections available was chosen for assessment. The procedure was modified slightly between brains from Experiment 1 and brains from Experiment 2 in order to account for the much lower background non-specific staining of the latter. For animals from Experiment 1, a $70 \times 70 \pm 2$ pixel box ($\sim 133 \times 133 \mu\text{m}$) was

created and a background measurement taken as far from the ME as it was possible to obtain in the captured field of view. Microscope light intensity was adjusted to standardize all background grayscale values to 85 ± 3 on a 1 to 256 intensity grayscale. The box was then dragged to Arc to obtain a measurement of the area of interest. The background value was subtracted from the value of the area of interest to obtain a relative fiber density measurement.

For animals from Experiment 2, a $70 \times 70 \pm 2$ pixel box ($\sim 133 \times 133 \mu\text{m}$) was created and a background measurement taken as far from the ME as it was possible in the captured field of view. Microscope light intensity was adjusted in order to standardize all background grayscale values to 65 ± 3 on a 1 to 256 intensity grayscale. The box was then dragged to Arc to obtain a measurement of the area of interest. The background value was subtracted from the value of the area of interest to obtain a relative fiber density measurement.

Statistical Analysis:

Data were analyzed using Statview SE + Graphics software (Abacus Concepts, Berkeley, CA) running on a Power Macintosh computer. In Experiment 1 we compared mean IR-GnRH neuron numbers between selected lines using Student's *t*-tests, with $P < 0.05$ as the level of significance. Comparisons between selected lines were carried out for the total number of neurons, for each individual brain structure where IR-cells were scored, and for the larger brain groups used for analysis of IR-cell distribution.

In Experiment 2 we compared mean IR-GnRH neuron numbers between selected lines and across photoperiod treatments using a 2-way ANOVA with $P < 0.05$ as the

level of significance. Comparisons across selected lines and photoperiod treatments were carried out for the total number of neurons, for each individual brain structure where IR-cells were scored, and for the larger brain groups used for analysis of IR-cell distribution. Bonferroni corrections were carried out on all individual brain structures with $P < 0.05$ according to a 2-way ANOVA. The Bonferroni correction is a multiple-comparison correction used when several independent statistical tests are being performed simultaneously. In order to avoid excessive spurious positives, the P -value for statistical significance needs to be adjusted to account for the number of comparisons being performed. A given P -value may be appropriate for each individual comparison, but not for the set of all comparisons. Brain structures were deemed to differ significantly between experimental groups when $P < 0.007$; since $P < \alpha/n$ where $\alpha = 0.05$ and $n =$ the number of brain structures having biologically relevant complements of IR-cells, arbitrarily set at an average of five for the four experimental groups. Nine such structures were found, and thus $P < 0.05 / 9 = 0.006$.

Because the mean number of IR-GnRH neurons might vary across ICC runs, we decided to account for any potential differences in the consistency of the procedure. Results from Experiment 2 were further analyzed using a 3-way ANOVA, where ICC run was a factor along with selection line and photoperiod treatment. We did not detect significant differences across ICC runs with this statistical test ($P = 0.958$; $F = 0.243$). A 1-way ANOVA with seven groups was also carried out in order to identify any significant differences that might be due to inconsistencies in our methods. This test also failed to detect significant differences across ICC runs ($P = 0.5093$; $F = 0.891$).

In Experiment 3 we compared mean relative fiber density between RM and NRM (animals from Experiment 1) at two different brain sites, using Student's *t*-tests with $P < 0.05$ as the level of significance. A 2-way ANOVA with a level of significance $P < 0.05$ was used to compare mean relative fiber density between selected lines and photoperiod treatments (animals from Experiment 2). Student's *t*-tests with $P < 0.05$ as the level of significance were used in within-lines comparisons of relative fiber density between photoperiod treatments in animals from Experiment 2.

Chapter 3 - Results:

Experiment 1:

We detected significantly ($P = 0.034$; $t = 2.326$) lower total numbers of immunoreactive GnRH neurons in the RM line (mean value = 101) than in the NRM line (mean value = 145) (Table 1; Figure 2a; Figure 3). In order to understand whether overall differences could be attributed to GnRH neurons in particular areas of the brain, individual structures and nuclei were combined into three groups for further analysis (Table 2). Significant differences in IR cell numbers between selection lines could be traced to the preoptic and anterior hypothalamic group ($P = 0.044$; $t = 2.194$; Preoptic/AH in Table 2; Figure 2c; Figure 3), which includes the medial and anteroventral preoptic areas (MPA/AVPO), periventricular hypothalamic nucleus (Pe), lateral preoptic area (LPO), median preoptic nucleus (MnPO), bed nucleus of the stria terminalis (BST), medial preoptic nucleus (MPO), anterior hypothalamic area – anterior (AHA), lateroanterior hypothalamic nucleus (LA), suprachiasmatic nucleus (SCh), and anterior amygdaloid area - ventral (AAV).

We did not detect significant differences in the number of IR-GnRH neurons between RM and NRM in the group of ventromedial brain structures and the lateral hypothalamus (Ventromedial/LH in Table 2; Figure 2d), which contains roughly the same number of IR cells as the Preoptic/AH group. IR-GnRH counts for this group of more-posterior GnRH neuron-containing regions, which includes the lateral hypothalamus (LH), tuber cinereum (TC), supraoptic nucleus, retrochiasmatic (SOR), optic tract (opt), supraoptic decussation (sox), ventromedial hypothalamic nucleus (VMH), arcuate

hypothalamic nucleus (Arc), median eminence (ME), and medial tuberal nucleus (Mtu), are similar in the two lines (Table 1; Figure 1d).

A group of anterior brain structures (Anterior in Table 2) that includes the lateral septal nucleus – intermediate (LSI/LS), olfactory tubercle and islands of Calleja (Tu/ICj), medial septal nucleus and lambdaoid septal zone (MS/Ld), vertical limb of the diagonal band of Broca (VDB), and horizontal limb of the diagonal band of Broca (HDB), had more IR-GnRH neurons in NRM than in RM, although the difference was not significant (Table 1; Figure 2b). However, when analyzed together with the Preoptic/AH group of structures, the selection lines differed significantly in the number of IR-GnRH neurons ($P = 0.023$; $t = 2.529$) (Table 1). Differences in IR-GnRH neuron numbers were not significant when major groups were combined in any other way (Table 1). No single brain nucleus or small region showed statistically significant differences in IR-GnRH cell numbers across selection lines (Table 2).

Experiment 2:

We detected significantly ($P < 0.001$; $F = 37.339$) lower total numbers of immunoreactive GnRH neurons in the RM line than in the NRM line (mean value = 109; RMLD mean value = 114; RMSD mean value = 104; NRM mean value = 173; NRMLD mean value = 176; NRMSD mean value = 169) (Table 3; Figure 4). We did not detect significant differences between mice raised in LD photoperiod (mean value = 145) and mice raised in SD photoperiod (mean value = 135; $P = 0.424$; $F = 0.650$).

IR-GnRH cells were scored in over one hundred different brain regions and nuclei (Table 3). Statistically significant differences ($P < 0.05$) between selected lines were

found in fifteen of these brain structures, while only one showed statistically significant differences between photoperiods (Table 3; Table 4). Given the large number of independent statistical tests performed simultaneously and a significance level of $P < 0.05$, approximately five of the significant differences found could result from chance alone. Bonferroni corrections to a lower P -value < 0.006 were carried out in order to detect potentially spurious positives. Brain structures were deemed to differ significantly if they met two criteria: a P – value < 0.006 , and an average of at least five neurons in the four experimental groups (Table 4).

Nine individual brain regions attained significant P – values after Bonferroni corrections: bed nucleus of the stria terminalis (BST; $P < 0.001$), horizontal limb of the diagonal band of Broca (HDB; $P = 0.002$), lateral preoptic area (LPO; $P < 0.001$), medial corticohypothalamic tract (mch; $P = 0.003$); medial and anteroventral preoptic areas (MPA/AVPO; $P = 0.001$), septohypothalamic nucleus (Shy; $P = 0.004$); olfactory tubercle and islands of Calleja (Tu/ICj; $P < 0.001$), vertical limb of the diagonal band of Broca (VDB; $P = 0.002$), and ventral pallidum (VP; $P = 0.001$). No single brain nucleus or small region showed statistically significant differences in IR-GnRH cell numbers between photoperiod treatments (Table 4). Of the nine regions with P – values < 0.006 , only five met the criteria for a biologically relevant neuron complement, arbitrarily set at an average of five for all experimental groups: HDB, LPO, MPA/AVPO, Tu/ICj, and VDB (Table 4).

In order to understand whether overall differences could be attributed to GnRH neurons in major spatial regions of the brain, individual structures and nuclei were combined into five groups representing spatial locations for further analysis (Table 5).

Significant differences across selection lines ($P = 0.006$; $F = 8.489$) but not between photoperiods ($P = 0.627$; $F = 0.240$) were found in a group that includes all IR-cells in the brain sections that correspond to plates 1 through 11 (Rostral in Table 5; Figure 5a) of the Paxinos and Watson atlas for the rat brain (1986). This group includes all the brain structures that are anterior to the fusion of the two halves of the corpus callosum.

Significant differences across selection lines ($P < 0.001$; $F = 21.507$) but not between photoperiods ($P = 0.987$; $F < 0.01$) were found in a group that includes all IR-cells found in the brain sections that correspond to plates 12 through 17 (Anterior in Table 5; Figure 5b) of the Paxinos and Watson atlas for the rat brain (1986). This group includes all brain structures posterior to the fusion of the two halves of the corpus callosum but anterior to the preoptic areas, such as the diagonal band of Broca, the medial septal nucleus, and most of the lateral septal nucleus. Significant differences across selection lines ($P < 0.001$; $F = 19.566$) but not between photoperiods ($P = 0.399$; $F = 0.723$) were also found in a group that includes all IR-cells found in the brain sections that correspond to plates 18 through 24 (Preoptic in Table 5; Figure 6a) of the Paxinos and Watson atlas for the rat brain (1986). This group includes all the preoptic areas, the most rostrally located parts of the anterior hypothalamic area, and the parts of the lateral hypothalamus that are anterior to the tuber cinereum.

We did not find significant differences between selection lines ($P = 0.064$; $F = 3.591$) or photoperiod treatments ($P = 0.321$; $F = 1.004$) in a group that includes all IR-cells in the brain sections that correspond to plates 25 through 32 (Posterior in Table 5; Figure 6b) of the Paxinos and Watson atlas for the rat brain (1986). This group includes all brain structures that appear rostrally along with the tuber cinereum, the median

eminence, most of the arcuate nucleus, as well as the entire ventromedial hypothalamus. We did not find significant differences across selection lines ($P = 0.091$; $F = 2.996$) or photoperiod treatments ($P = 0.792$; $F = 0.071$) in a group that includes all IR-cells in the brain sections that correspond to plate 33 and all plates posterior to plate 33 (Caudal in Table 5; Figure 7) of the Paxinos and Watson atlas for the rat brain (1986). This group includes the more caudal portions of the lateral hypothalamus, but does not contain any portions of the ventromedial hypothalamus.

We detected significant differences in paired testis mass between selected lines ($P < 0.001$; $F = 56.944$) and between photoperiod treatments ($P < 0.001$; $F = 72.062$) (Table 6; Figure 8a). In addition, we found significant differences in paired seminal vesicle mass between selected lines ($P < 0.001$; $F = 32.42$) as well as between photoperiod treatments ($P < 0.001$; $F = 73.84$) (Table 6; Figure 8b). We did not detect statistically significant differences in body mass between selected lines ($P = 0.109$; $F = 2.664$) or between photoperiods ($P = 0.122$; $F = 2.474$) (Table 6; Figure 8c).

Experiment 3:

We did not detect statistically significant differences in AMPO relative fiber density ($P = 0.229$; $F = 1.570$) between RM and NRM from Experiment 1 (Table 7). Similarly, we did not detect statistically significant differences in Arc/ME relative fiber density ($P = 0.675$; $F = 0.183$) between RM and NRM from Experiment 1 (Table 7). We did not find differences in AMPO relative fiber densities between selected lines ($P = 0.156$; $F = 2.077$) or photoperiods ($P = 0.067$; $F = 3.494$) in mice from Experiment 2 (Table 8). We did find significant differences in Arc/ME relative fiber density ($P < 0.001$;

$F = 36.040$) between mice raised in SD photoperiod and mice raised in LD photoperiod (Table 8), but did not find statistically significant differences between selected lines ($P = 0.229$; $F = 1.480$). RM-only relative fiber density comparisons between photoperiod treatments indicated significant differences between RMLD and RMSD at both the AMPO ($P = 0.030$) and the Arc ($P < 0.001$) (Table 9). NRM-only relative fiber density comparisons between photoperiod treatments indicated statistically significant differences observed at the Arc ($P = 0.015$), but not at the AMPO ($P = 0.688$) (Table 10).

Table 1: Mean number of immunoreactive GnRH neurons. Data are organized by brain groups defined in text and Table 2. Values are expressed as mean \pm S.E.M, with attained P-values for differences between lines.

Group	RM mean value	NRM mean value	P - Value
Anterior	33.9 \pm 4.9	51.0 \pm 7.9	0.094
Preoptic/AH	31.0 \pm 4.8	55.6 \pm 9.6	0.044
Ventromedial/LH	31.0 \pm 4.0	36.0 \pm 5.8	0.501
Combined Anterior + Preoptic/AH	64.9 \pm 7.0	106.6 \pm 14.2	0.023
Combined Anterior + Ventromedial/LH	64.9 \pm 6.8	87.0 \pm 8.4	0.061
Combined Preoptic/AH + Ventromedial/LH	62.0 \pm 7.2	91.6 \pm 12.6	0.067
Total	100.8 \pm 9.9	145.4 \pm 15.8	0.034

Table 2: Mean number of immunoreactive GnRH neurons. Data are organized by their assigned brain region and values are expressed as mean \pm S.E.M. Abbreviations are from Paxinos and Watson (1986).

Group	Brain Region	RM (n = 8)	NRM (n =9)
Anterior	LSI/LS	4.6 \pm 0.8	8.1 \pm 1.6
Anterior	Tu/ICj	1.4 \pm 1.1	2.0 \pm 0.7
Anterior	MS/Ld	1.4 \pm 0.5	1.3 \pm 0.5
Anterior	VDB	19.4 \pm 3.8	28.0 \pm 5.5
Anterior	HDB	7.1 \pm 2.4	11.6 \pm 2.8
Preoptic/AH	MPA/AVPO	17.4 \pm 3.0	28.9 \pm 6.2
Preoptic/AH	Pe	0.4 \pm 0.2	1.0 \pm 0.3
Preoptic/AH	LPO	6.0 \pm 2.1	11.7 \pm 2.6
Preoptic/AH	MnPO	0.1 \pm 0.1	0.8 \pm 0.5
Preoptic/AH	BST	3.3 \pm 0.1	5.8 \pm 1.3
Preoptic/AH	MPO	1.0 \pm 0.5	0.8 \pm 0.4
Preoptic/AH	AHA	0.4 \pm 0.2	1.1 \pm 0.5
Preoptic/AH	LA	2.0 \pm 0.6	4.3 \pm 1.4
Preoptic/AH	SCh	0.1 \pm 0.1	0.7 \pm 0.3
Preoptic/AH	AAV	0.4 \pm 0.2	0.6 \pm 0.4
Ventromedial/LH	LH	10.5 \pm 1.7	11.4 \pm 1.8
Ventromedial/LH	TC/SOR	12.8 \pm 1.7	16.0 \pm 4.1
Ventromedial/LH	opt/sox	1.1 \pm 0.7	0.4 \pm 0.2
Ventromedial/LH	VMH	2.6 \pm 0.9	2.9 \pm 1.0
Ventromedial/LH	Arc/ME	1.4 \pm 0.5	2.1 \pm 0.5
Ventromedial/LH	MTu	2.6 \pm 1.0	3.1 \pm 1.6
	Total	100.8 \pm 9.9	145.4 \pm 15.8

Figure 2: Mean number of IR-GnRH neurons in RM (n = 8) and NRM (n = 9) from Experiment 1 (SD). Data are organized by group: Total (a); Anterior (b); Preoptic/AH (c); Ventromedial/LH (d). Error bars: S.E.M.

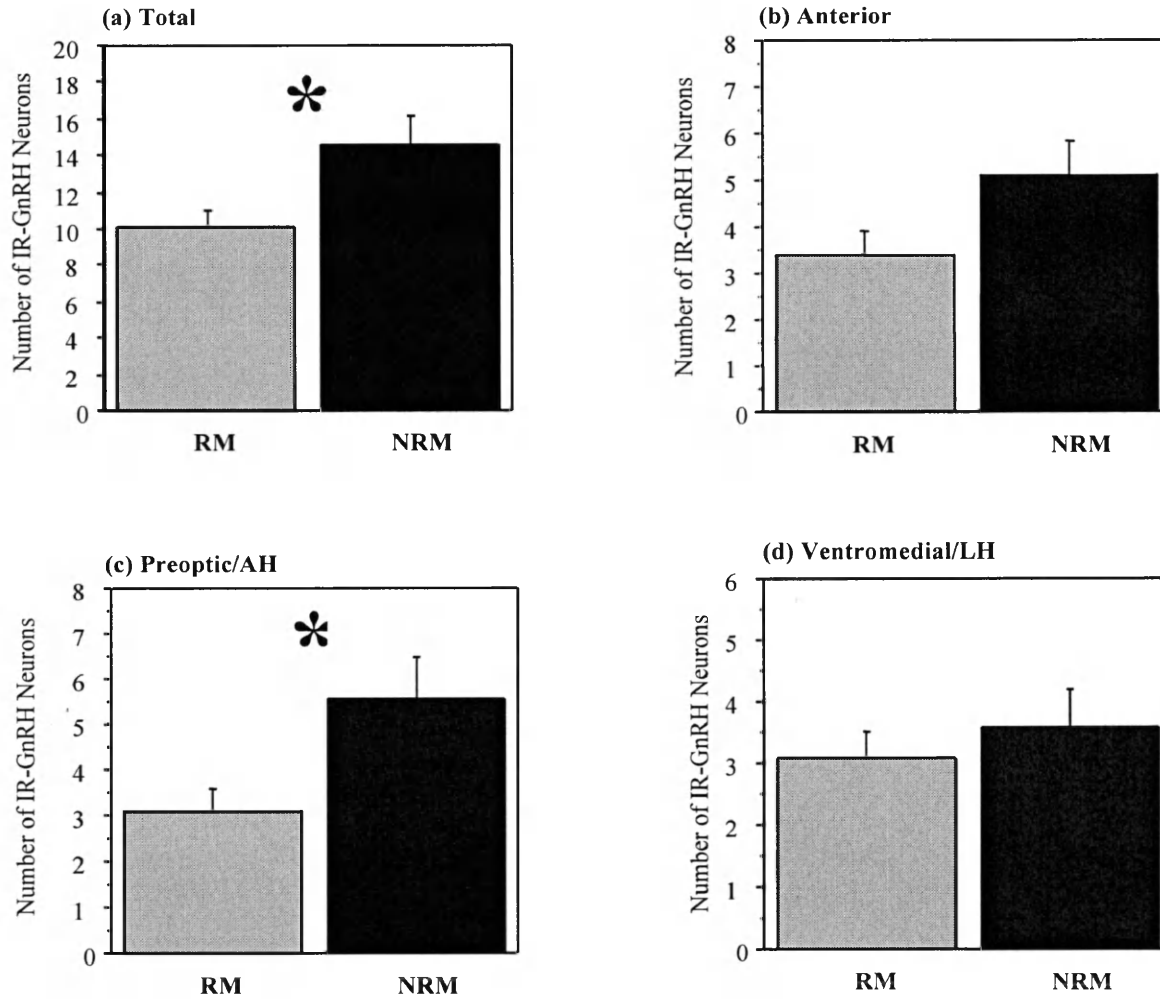


Figure 3: Representative coronal sections from RM (a) and NRM (b) from Experiment 1, both with numbers of IR-GnRH neurons near the mean for their group. The medial preoptic area is enclosed within the dashed line, and arrow heads indicate cells with GnRH-like immunocytochemistry. Abbreviations: MPA – medial preoptic area; AVPO – anteroventral preoptic area; ox – optic chiasm.

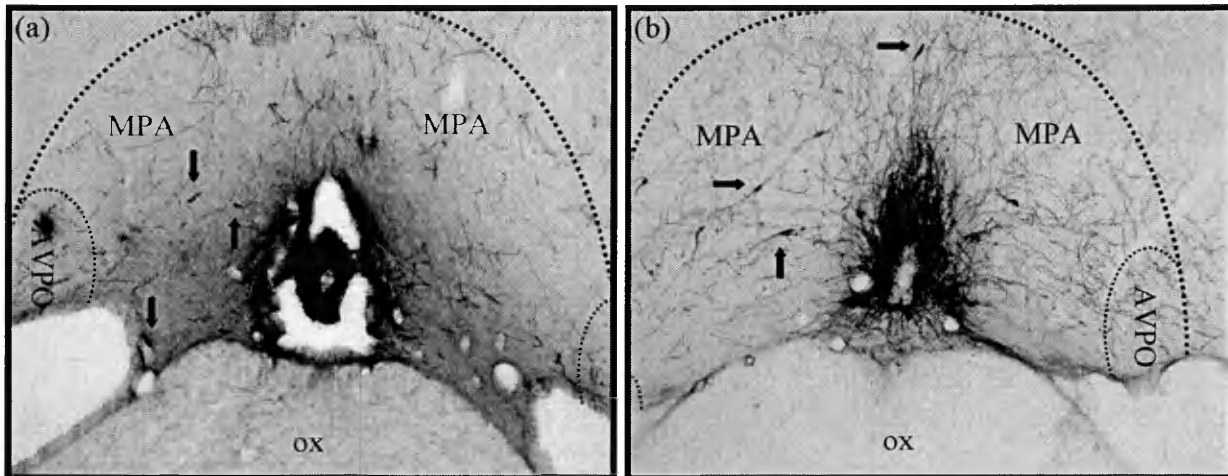


Table 3: Mean number of immunoreactive GnRH neurons. Data are organized by their assigned brain region and values are expressed as mean \pm S.E.M. Abbreviations are from Paxinos and Watson (1986). Brain regions exhibiting P – values < 0.05 are identified with an asterisk (*), and attained P – values are stated.

Brain Region	RMLD (n = 14)	RMSD (n = 14)	NRMLD (n = 14)	NRMSD (n = 13)	P - Value
AA	0.1 \pm 0.1	0.1 \pm 0.1	0.2 \pm 0.1	0.1 \pm 0.1	
AAD (* photoperiod)	0.1 \pm 0.1	0.1 \pm 0.1	0.6 \pm 0.2	0.0 \pm 0.0	0.018
AASh	0.4 \pm 0.2	0.1 \pm 0.1	0.0 \pm 0.0	0.2 \pm 0.1	
AAV	3.6 \pm 0.7	1.9 \pm 0.4	1.9 \pm 0.5	2.3 \pm 0.5	
AC	0.0 \pm 0.0	0.0 \pm 0.0	0.0 \pm 0.0	0.1 \pm 0.1	
Acb	0.0 \pm 0.0	0.0 \pm 0.0	0.1 \pm 0.1	0.2 \pm 0.1	
AcbC	0.0 \pm 0.0	0.1 \pm 0.1	0.0 \pm 0.0	0.2 \pm 0.2	
AcbSh	0.5 \pm 0.3	0.2 \pm 0.1	0.3 \pm 0.2	0.5 \pm 0.2	
ACo	0.2 \pm 0.1	0.4 \pm 0.3	0.2 \pm 0.2	0.2 \pm 0.2	
AHA (* line)	0.6 \pm 0.2	0.5 \pm 0.2	1.1 \pm 0.2	1.8 \pm 0.7	0.023
AHC	0.3 \pm 0.1	0.3 \pm 0.1	0.5 \pm 0.2	0.2 \pm 0.1	
AHP	0.1 \pm 0.1	0.3 \pm 0.2	0.2 \pm 0.1	0.4 \pm 0.1	
AMPO	1.4 \pm 0.7	0.7 \pm 0.3	0.6 \pm 0.3	1.0 \pm 0.3	
AOP	0.1 \pm 0.1	0.0 \pm 0.0	0.0 \pm 0.0	0.0 \pm 0.0	
Arc/ME	1.1 \pm 0.3	1.3 \pm 0.5	2.0 \pm 0.5	1.4 \pm 0.8	
BAOT	0.3 \pm 0.2	0.1 \pm 0.1	0.1 \pm 0.1	0.3 \pm 0.2	
BM	0.0 \pm 0.0	0.0 \pm 0.0	0.0 \pm 0.0	0.1 \pm 0.1	
BMA	0.1 \pm 0.1	0.0 \pm 0.0	0.1 \pm 0.1	0.0 \pm 0.0	
BST (* line)	2.0 \pm 0.4	1.1 \pm 0.4	4.5 \pm 0.9	3.5 \pm 0.6	<0.001
Cg1	0.0 \pm 0.0	0.0 \pm 0.0	0.0 \pm 0.0	0.2 \pm 0.1	
Cg2	0.0 \pm 0.0	0.0 \pm 0.0	0.0 \pm 0.0	0.1 \pm 0.1	
Cp	0.0 \pm 0.0	0.1 \pm 0.1	0.0 \pm 0.0	0.0 \pm 0.0	
CPu	0.1 \pm 0.1	0.0 \pm 0.0	0.0 \pm 0.0	0.2 \pm 0.2	
CxA (* line)	0.6 \pm 0.2	0.0 \pm 0.0	1.3 \pm 0.5	0.6 \pm 0.3	0.037
DA	0.1 \pm 0.1	0.0 \pm 0.0	0.1 \pm 0.1	0.1 \pm 0.1	
DM	0.2 \pm 0.1	0.0 \pm 0.0	0.1 \pm 0.1	0.2 \pm 0.1	
DMC	0.1 \pm 0.1	0.0 \pm 0.0	0.0 \pm 0.0	0.0 \pm 0.0	
DMD	0.1 \pm 0.1	0.0 \pm 0.0	0.2 \pm 0.2	0.2 \pm 0.2	
DP	0.1 \pm 0.1	0.0 \pm 0.0	0.4 \pm 0.2	0.2 \pm 0.2	
F	0.1 \pm 0.1	0.0 \pm 0.0	0.2 \pm 0.2	0.1 \pm 0.1	
FSTr	0.1 \pm 0.1	0.0 \pm 0.0	0.1 \pm 0.1	0.0 \pm 0.0	

Gcc	0.0 ± 0.0	0.0 ± 0.0	0.0 ± 0.0	0.2 ± 0.2	
HDB (* line)	8.1 ± 1.1	7.4 ± 1.6	12.1 ± 1.2	13.4 ± 2.1	0.002
IG	0.1 ± 0.1	0.0 ± 0.0	0.1 ± 0.1	0.8 ± 0.8	
IL	0.0 ± 0.0	0.0 ± 0.0	0.0 ± 0.0	0.1 ± 0.1	
InfS	0.0 ± 0.0	0.0 ± 0.0	0.1 ± 0.1	0.0 ± 0.0	
Io	0.7 ± 0.3	0.1 ± 0.1	0.5 ± 0.2	0.9 ± 0.5	
LA	0.9 ± 0.4	0.6 ± 0.3	0.8 ± 0.3	0.9 ± 0.3	
LH (* line)	11.9 ± 2.4	8.5 ± 1.4	17.1 ± 2.9	14.5 ± 2.1	
LM	0.0 ± 0.0	0.1 ± 0.1	0.1 ± 0.1	0.1 ± 0.1	
LOT	0.7 ± 0.4	0.4 ± 0.2	0.8 ± 0.2	0.5 ± 0.3	
LPO (* line)	8.9 ± 1.3	10.6 ± 1.6	18.4 ± 1.7	16.9 ± 1.6	<0.001
LSD	0.1 ± 0.1	0.0 ± 0.0	0.0 ± 0.0	0.1 ± 0.1	
LSI (* line)	7.6 ± 1.9	5.7 ± 0.9	10.6 ± 1.2	9.1 ± 1.6	0.032
LSV	0.2 ± 0.2	0.1 ± 0.1	0.2 ± 0.1	0.3 ± 0.1	
mch (* line)	0.1 ± 0.1	0.1 ± 0.1	0.6 ± 0.2	0.5 ± 0.2	0.003
MCLH	0.0 ± 0.0	0.0 ± 0.0	0.0 ± 0.0	0.1 ± 0.1	
MCPO (* line)	0.6 ± 0.2	0.9 ± 0.3	0.2 ± 0.1	0.3 ± 0.2	0.014
MeA	0.2 ± 0.2	0.4 ± 0.4	0.1 ± 0.1	0.3 ± 0.2	
MeAD	0.4 ± 0.2	0.0 ± 0.0	0.0 ± 0.0	0.2 ± 0.1	
MeAV	0.1 ± 0.1	0.1 ± 0.1	0.0 ± 0.0	0.0 ± 0.0	
MePD	0.0 ± 0.0	0.0 ± 0.0	0.1 ± 0.1	0.1 ± 0.1	
MePV	0.1 ± 0.1	0.1 ± 0.1	0.1 ± 0.1	0.2 ± 0.1	
MnPO	1.1 ± 0.5	1.4 ± 0.4	1.5 ± 0.3	1.7 ± 0.5	
MP	0.0 ± 0.0	0.1 ± 0.1	0.0 ± 0.0	0.0 ± 0.0	
Mp	0.0 ± 0.0	0.0 ± 0.0	0.1 ± 0.1	0.0 ± 0.0	
MPA/AVPO (* line)	17.0 ± 2.0	15.1 ± 2.1	24.6 ± 3.2	25.5 ± 2.4	0.001
MPO	0.3 ± 0.2	0.4 ± 0.2	0.8 ± 0.3	0.5 ± 0.2	
MS/Ld	3.8 ± 0.8	3.8 ± 1.0	5.6 ± 1.3	5.5 ± 1.0	
Mtu	2.0 ± 0.6	2.0 ± 0.7	5.0 ± 1.4	2.9 ± 1.0	
Opt/sox	3.0 ± 0.7	2.6 ± 0.6	1.9 ± 0.5	2.5 ± 0.6	
OX	0.0 ± 0.0	0.1 ± 0.1	0.1 ± 0.1	0.1 ± 0.1	
PaAP	0.1 ± 0.1	0.1 ± 0.1	0.1 ± 0.1	0.1 ± 0.1	
PaLM	0.0 ± 0.0	0.1 ± 0.1	0.0 ± 0.0	0.0 ± 0.0	
PaPO	0.0 ± 0.0	0.0 ± 0.0	0.0 ± 0.0	0.1 ± 0.1	
PaV	0.0 ± 0.0	0.1 ± 0.1	0.1 ± 0.1	0.1 ± 0.1	
Pe	0.9 ± 0.3	0.6 ± 0.2	0.6 ± 0.2	1.3 ± 0.3	
PeF	0.0 ± 0.0	0.0 ± 0.0	0.1 ± 0.1	0.0 ± 0.0	

PH	0.1 ± 0.1	0.0 ± 0.0	0.4 ± 0.2	0.0 ± 0.0	
Pir	0.1 ± 0.1	0.2 ± 0.1	0.2 ± 0.1	0.2 ± 0.2	
PLd	0.0 ± 0.0	0.1 ± 0.1	0.0 ± 0.0	0.0 ± 0.0	
PMD	0.0 ± 0.0	0.0 ± 0.0	0.2 ± 0.2	0.0 ± 0.0	
PMV	0.1 ± 0.1	0.1 ± 0.1	0.2 ± 0.2	0.2 ± 0.2	
PS	0.0 ± 0.0	0.0 ± 0.0	0.0 ± 0.0	1.6 ± 1.5	
RCh	0.1 ± 0.1	0.0 ± 0.0	0.1 ± 0.1	0.1 ± 0.1	
RE	0.0 ± 0.0	0.0 ± 0.0	0.1 ± 0.1	0.0 ± 0.0	
RF	0.1 ± 0.1	0.0 ± 0.0	0.0 ± 0.0	0.0 ± 0.0	
SCh	0.7 ± 0.7	0.7 ± 0.7	0.7 ± 0.7	0.4 ± 0.2	
SFi	0.0 ± 0.0	0.0 ± 0.0	0.0 ± 0.0	0.1 ± 0.1	
SFO	0.0 ± 0.0	0.1 ± 0.1	0.0 ± 0.0	0.1 ± 0.1	
SHi	0.6 ± 0.3	0.0 ± 0.0	0.4 ± 0.2	0.2 ± 0.1	
SHy (* line)	0.2 ± 0.2	0.2 ± 0.1	1.6 ± 0.7	1.0 ± 0.2	0.004
SI	0.1 ± 0.1	0.1 ± 0.1	0.4 ± 0.3	0.2 ± 0.2	
SO	1.2 ± 0.5	1.8 ± 0.4	1.2 ± 0.4	1.6 ± 0.4	
Sta	0.0 ± 0.0	0.0 ± 0.0	0.1 ± 0.1	0.1 ± 0.1	
StHy	0.3 ± 0.2	0.1 ± 0.1	0.3 ± 0.2	0.1 ± 0.1	
TC/SOR (* line)	9.4 ± 1.4	10.2 ± 1.5	16.2 ± 2.5	10.8 ± 1.1	0.038
Te	0.1 ± 0.1	0.4 ± 0.2	0.1 ± 0.1	0.1 ± 0.1	
TM	0.0 ± 0.0	0.0 ± 0.0	0.1 ± 0.1	0.1 ± 0.1	
TS	0.1 ± 0.1	0.0 ± 0.0	0.0 ± 0.0	0.0 ± 0.0	
TT	0.6 ± 0.2	0.4 ± 0.3	1.4 ± 0.6	1.5 ± 0.8	
Tu/ICj (* line)	4.3 ± 0.8	3.7 ± 0.6	6.7 ± 0.9	9.1 ± 1.6	<0.001
Vaf	0.0 ± 0.0	0.0 ± 0.0	0.0 ± 0.0	0.1 ± 0.1	
VDB (* line)	13.1 ± 2.2	15.1 ± 3.0	23.6 ± 2.8	22.1 ± 2.5	0.002
VEn	0.1 ± 0.1	0.0 ± 0.0	0.3 ± 0.2	0.2 ± 0.1	
VM	0.0 ± 0.0	0.0 ± 0.0	0.0 ± 0.0	0.2 ± 0.2	
VMH	1.1 ± 1.3	1.1 ± 0.3	1.8 ± 0.5	1.8 ± 0.6	
VP (* line)	1.0 ± 0.3	1.6 ± 0.4	3.1 ± 0.6	3.8 ± 1.0	0.001
ZI	0.0 ± 0.0	0.0 ± 0.0	0.1 ± 0.1	0.0 ± 0.0	
Total	113.9 ± 10.9	103.6 ± 9.6	175.8 ± 11.7	169.3 ± 9.2	

Table 4: Bonferroni corrections for brain regions with P – values < 0.05 according to a 2-way ANOVA. Brain regions were deemed to differ significantly if they possessed a biologically relevant number of neurons (see text) and attained P – values of < 0.006 . Regions meeting both criteria are identified with an asterisk (*). Data are organized by their assigned brain region. Abbreviations are from Paxinos and Watson (1986).

Brain Region	Effect	ANOVA P -value	Bonferroni Correction ($P < 0.006$)
AAD	Photoperiod	0.018	
AHA	Line	0.023	
BST	Line	< 0.001	
CxA	Line	0.037	
HDB	Line	0.002	*
LH	Line	0.019	
LPO	Line	< 0.001	*
LSI	Line	0.032	
mch	Line	0.003	
MCPO	Line	0.014	
MPA/AVPO	Line	0.001	*
SHy	Line	0.004	
TC/SOR	Line	0.038	
Tu/ICj	Line	< 0.001	*
VDB	Line	0.002	*
VP	Line	0.001	

Table 5: Mean number of immunoreactive GnRH neurons. Data are organized by brain groups defined in text. Values are expressed as mean \pm S.E.M, with attained P-values for differences between lines and photoperiods. Brain groups exhibiting statistically significant differences after Bonferroni corrections are identified with an asterisk (*). Bonferroni correction: $P < \alpha/n$ where $\alpha = 0.05$ and $n = 5$. $P < 0.01$

Group	RMLD mean value	RMSD mean value	NRMLD mean value	NRMSD mean value	Photoperiod <i>P</i> - Value	Line <i>P</i> - Value	Bonferroni Correction ($P < 0.01$)
Rostral	4.3 \pm 1.2	4.7 \pm 0.8	8.2 \pm 1.8	9.2 \pm 1.8	0.627	0.006	*
Anterior	33.4 \pm 3.5	32.5 \pm 5.3	55.2 \pm 5.4	56.2 \pm 5.3	0.987	<0.001	*
Preoptic	55.2 \pm 6.8	46.3 \pm 4.6	79.6 \pm 7.7	77.8 \pm 5.6	0.399	<0.001	*
Posterior	21.2 \pm 3.6	19.9 \pm 3.3	31.6 \pm 5.5	24.8 \pm 3.4	0.321	0.064	
Caudal	0.7 \pm 0.3	2.0 \pm 0.6	4.4 \pm 2.0	2.5 \pm 0.9	0.792	0.091	
Total	113.9 \pm 10.9	103.6 \pm 9.6	175.8 \pm 11.7	169.3 \pm 9.2	0.424	<0.001	*

Figure 4: Mean total number of IR-GnRH neurons in RMLD (n = 14), NRMLD (n = 14), RMSD (n = 14), and NRMSD (n = 13) from Experiment 2. Error bars: S.E.M.

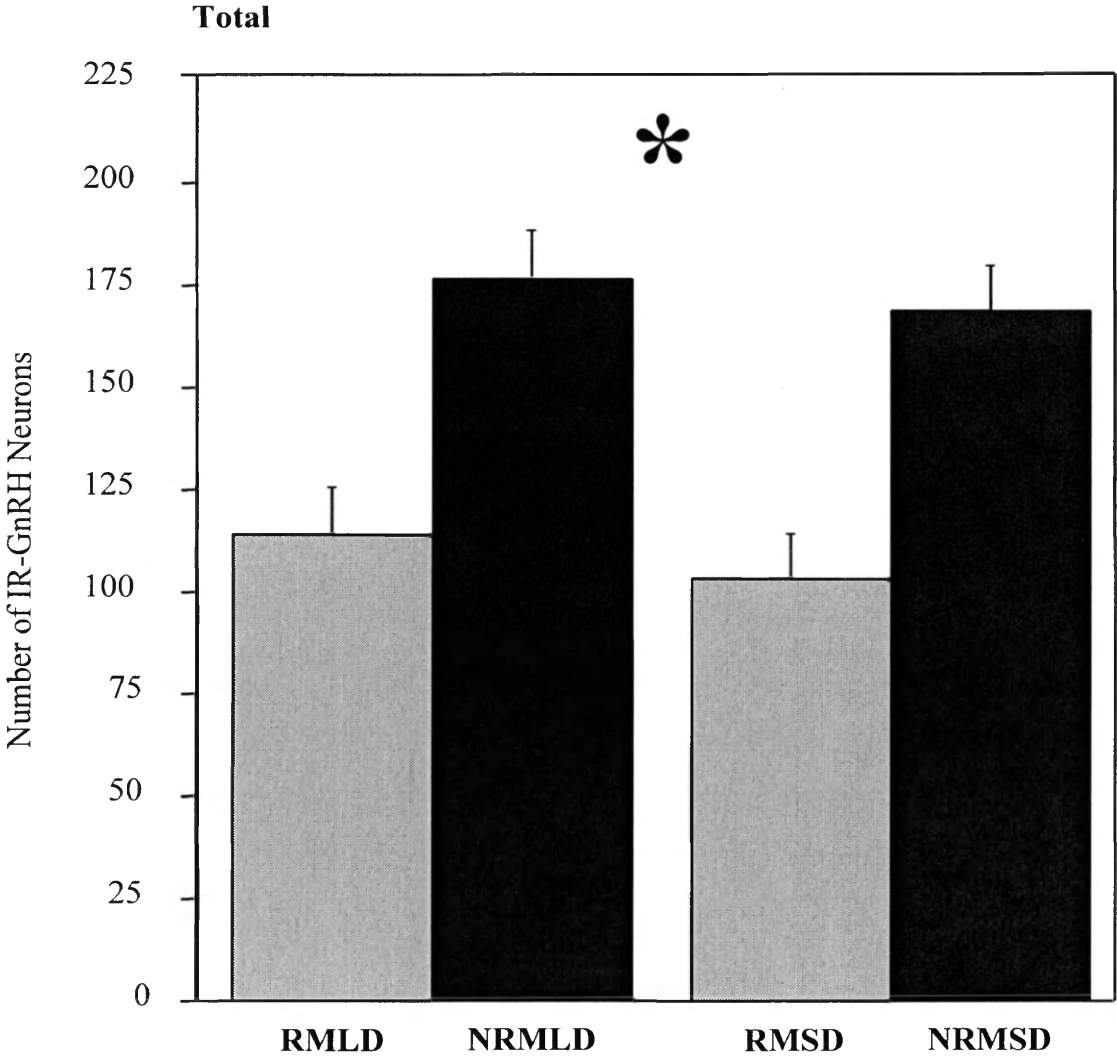


Figure 5: Mean number of IR-GnRH neurons in RM and NRM from Experiment 2. Data are organized by group. Rostral (a): RMLD (n = 12), NRMLD (n = 11), RMSD (n = 10), and NRMSD (n = 9). Anterior (b): RMLD (n = 14), NRMLD (n = 14), RMSD (n = 14), and NRMSD (n = 13). Error bars: S.E.M.

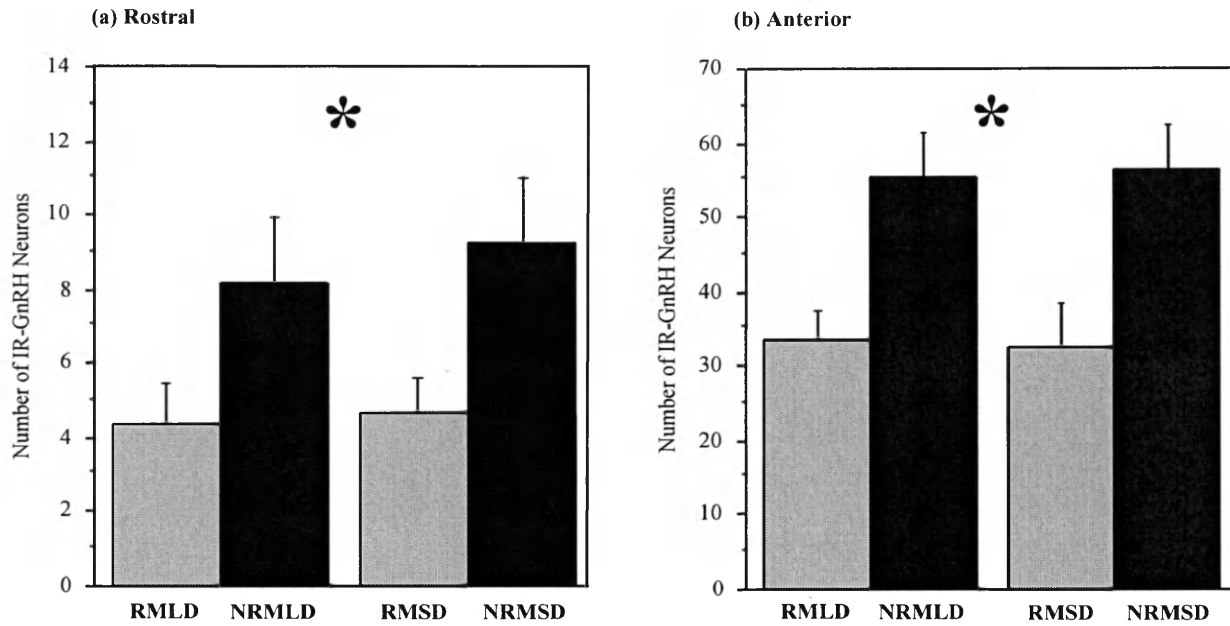


Figure 6: Mean number of IR-GnRH neurons in RMLD (n = 14), NRMLD (n = 14), RMSD (n = 14), and NRMSD (n = 13) from Experiment 2. Data are organized by group: Preoptic (a) and Posterior (b). Error bars: S.E.M.

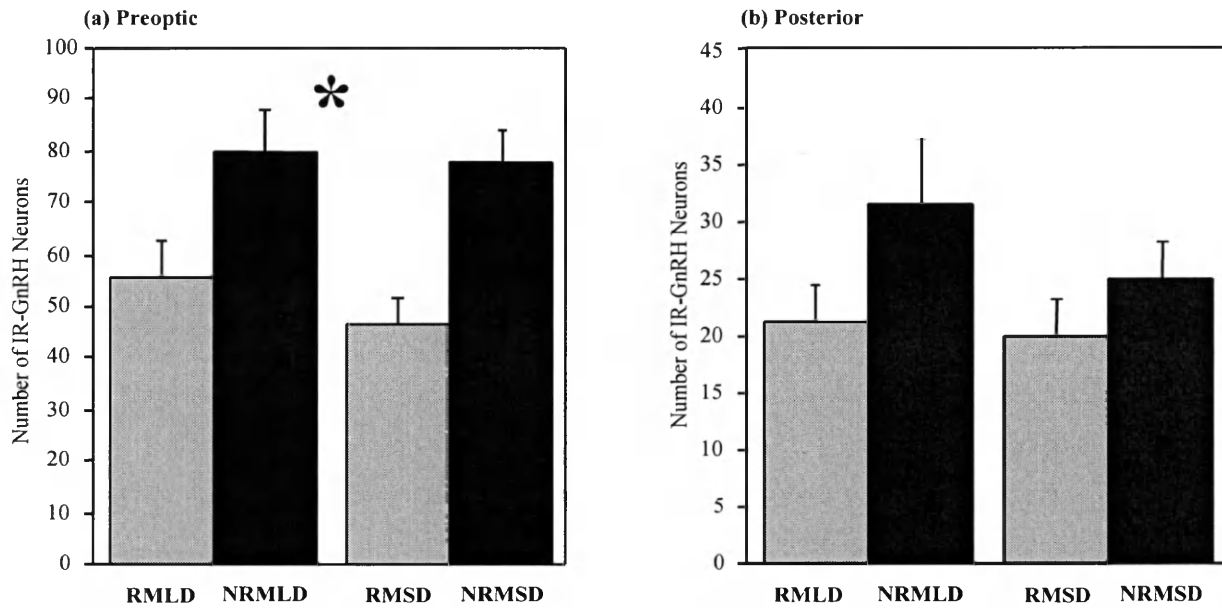


Figure 7: Mean number of IR-GnRH neurons in RM and NRM, group Caudal, Experiment 2. RMLD (n = 11), NRMLD (n = 12), RMSD (n = 12), and NRMSD (n = 10) from Experiment 2. Error bars: S.E.M.

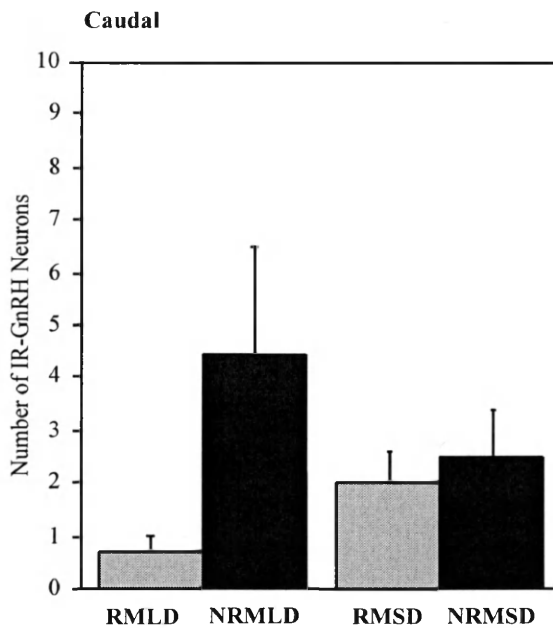


Table 6: Mean testis, seminal vesicle (SV), and body masses of RM and NRM from Experiment 2. Values are expressed as mean \pm S.E.M., with attained P-values for differences between lines and photoperiods.

Mass (grams)	RMLD mean value	RMSD mean value	NRMLD mean value	NRMSD mean value	Line P - Value	Photoperiod P - Value
Paired Testis	0.29 \pm 0.02	0.08 \pm 0.01	0.46 \pm 0.02	0.27 \pm 0.03	< 0.001	< 0.001
Paired SV	0.17 \pm 0.02	0.01 \pm 0	0.34 \pm 0.03	0.10 \pm 0.08	< 0.001	< 0.001
Intact Body	20.05 \pm 0.82	18.01 \pm 0.74	20.68 \pm 0.71	20.10 \pm 1.05	0.109	0.122

Figure 8: Mean paired testis mass, mean paired seminal vesicle mass, and mean body mass of RM and NRM is SD and LD. Within-lines changes in the reproductive axis between photoperiods appear to be independent of changes in number and location of IR-GnRH neurons. Error bars: S.E.M.

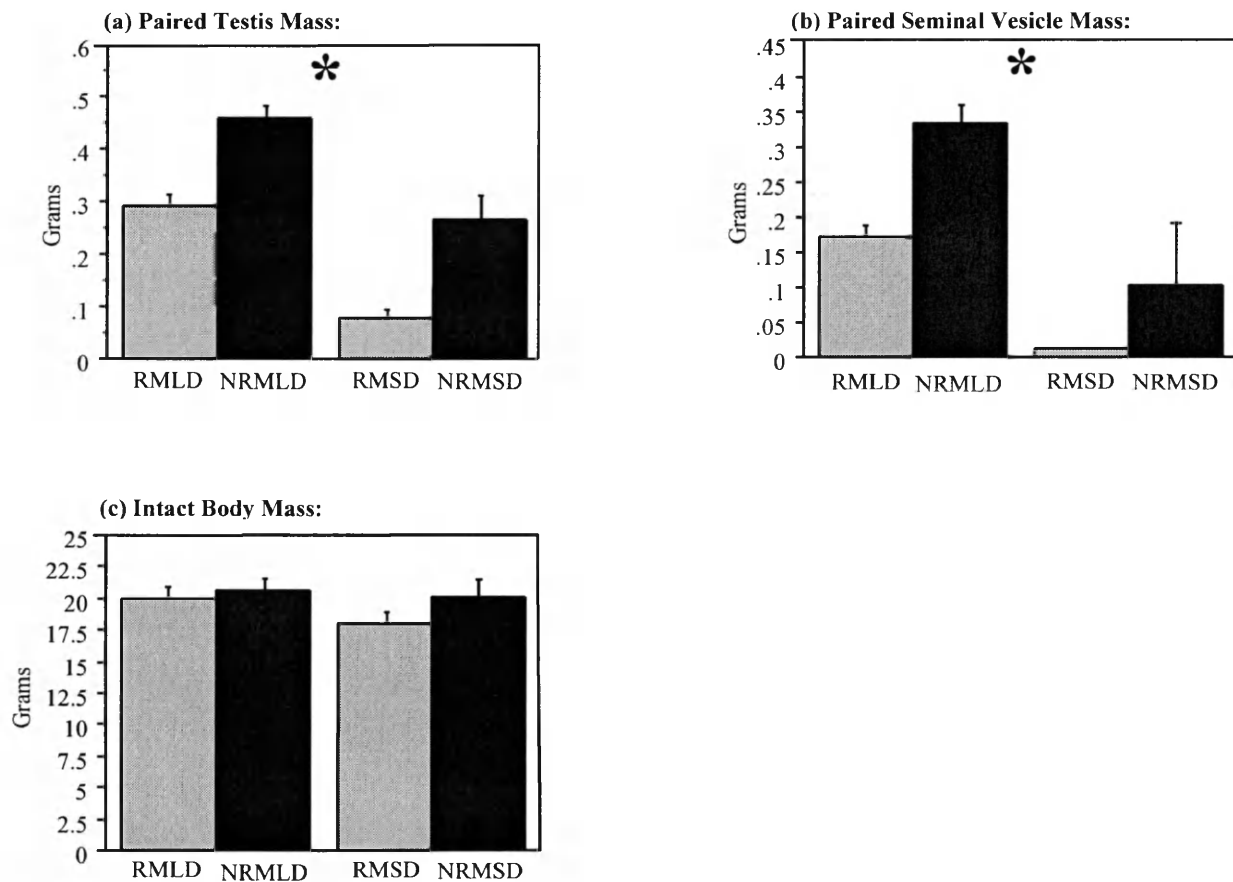


Figure 9: 1 factor ANOVA for 7 groups. No statistically significant differences in the number of IR-GnRH perykarya were detected across ICC runs. Error Bars: 95% Confidence Interval.

	Brains used	Mean IR-cell count	Std. Dev.	S.E.M
Run 1	5	128.0	45.371	20.290
Run 2	7	145.7	34.413	13.007
Run 3	12	123.6	67.350	19.442
Run 4	5	115.2	57.352	25.648
Run 5	9	151.0	37.832	12.611
Run 6	10	162.2	54.401	17.203
Run 7	7	143.9	24.802	9.374

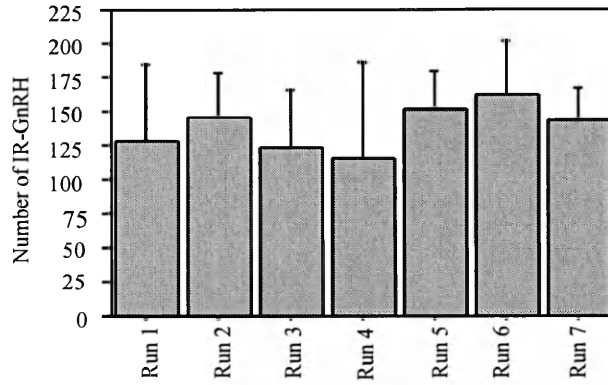


Table 7: Mean relative fiber density values by experimental group, RM and NRM from Experiment 1. Values are expressed as mean \pm S.E.M., with attained P-values for differences between lines and photoperiods.

Brain Region	RM mean value	NRM mean value	Line P - Value
AMPO	25.7 \pm 7.0	41.3 \pm 9.9	0.229
Arc	129.8 \pm 3.8	131.5 \pm 1.6	0.675

Figure 10: Relative GnRH fiber density in RM (n = 8) and NRM (n = 9) from Experiment 1. Data are organized by brain structure: AMPO (a) and Arc (b). Error bars: S.E.M.

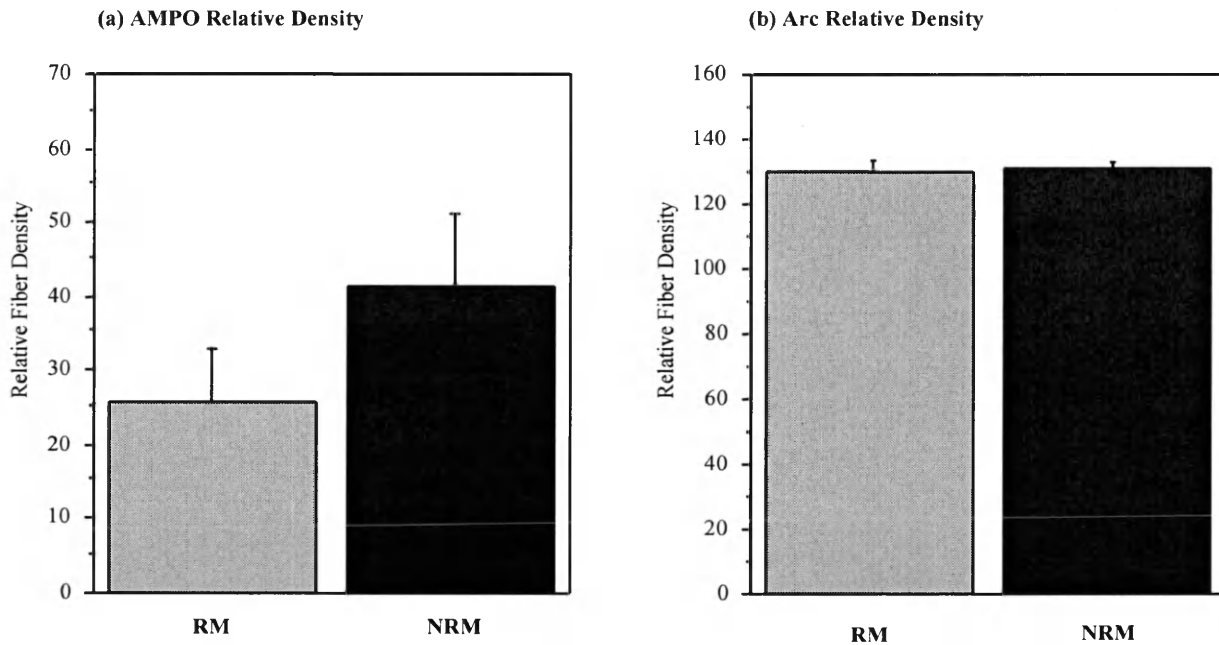


Table 8: Mean relative fiber density values by experimental group, mice from Experiment 2. Values are expressed as mean \pm S.E.M., with attained P-values for differences between lines and photoperiods.

Brain Region	RMLD mean value	RMSD mean value	NRMLD mean value	NRMSD mean value	Line P - Value	Photoperiod P - Value
AMPO	37.1 \pm 5.7	21.6 \pm 3.6	23.7 \pm 4.6	20.1 \pm 5.5	0.156	0.067
Arc	94.1 \pm 6.9	51.7 \pm 2.6	75.8 \pm 4.3	57.7 \pm 5.4	0.229	<0.001

Figure 11: Relative GnRH fiber density in RMLD (n = 14), NRMLD (n = 14), RMSD (n = 14), and NRMSD (n = 13) from Experiment 2. Data are organized by brain structure: AMPO (a) and Arc (b). Error bars: S.E.M.

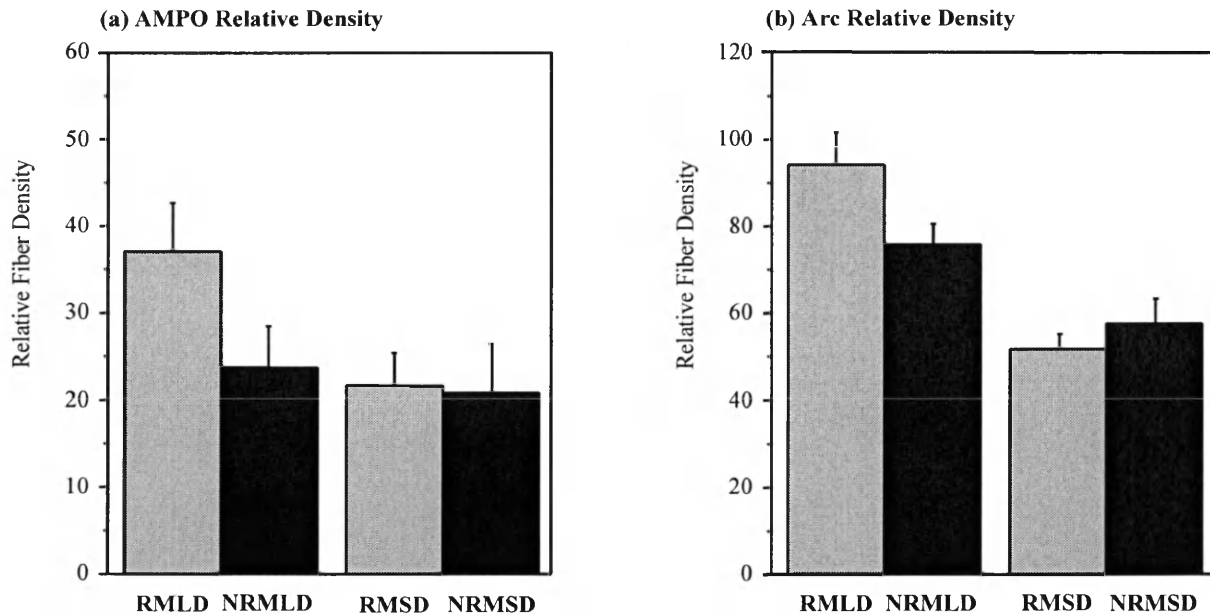


Table 9: RM mean relative fiber density values, RMLD and RMSD from Experiment 2. Values are expressed as mean \pm S.E.M., with attained P-values for differences between lines and photoperiods.

Brain Region	RMLD mean value	RMSD mean value	<i>P</i> - Value
AMPO	37.1 \pm 5.7	21.6 \pm 3.6	0.030
Arc	94.1 \pm 6.9	51.7 \pm 2.6	< 0.001

Table 10: NRM mean relative fiber density values, NRMLD and NRMSD from Experiment 2. Values are expressed as mean \pm S.E.M., with attained P-values for differences between lines and photoperiods.

Brain Region	NRMLD mean value	NRMSD mean value	<i>P</i> - Value
AMPO	23.7 \pm 4.6	20.1 \pm 5.5	0.688
Arc	75.8 \pm 4.3	57.7 \pm 5.4	0.015

Chapter 4 - Discussion:

Our data are consistent with the hypothesis that within-species variation in photoperiod responsiveness is due in part to variation in GnRH neuronal activity. *P. leucopus* selected to retain year-round reproductive competence possess a larger complement of mature GnRH-releasing cells in SD and LD than mice selected to experience reproductive inhibition. Our results from Experiment 1 are consistent with previous findings obtained in an unselected but phenotypically diverse colony of *P. maniculatus* tested in SD only (Korytko et al., 1995; Korytko et al., 1997; Korytko et al., 1998). In addition, our results are consistent with and extend the conclusions from previous experiments on unselected female *P. leucopus* from a different locality, where variation in photoperiod responsiveness was found to correlate with variation in GnRH cell numbers and location in SD (Glass, 1986).

Two major differences from previous immunocytochemical studies comparing GnRH neurons of photoperiod responsive and photoperiod nonresponsive *Peromyscus spp.* allow for important new conclusions to be reached. First, the antibody used here preferentially binds mature GnRH rather than prohormone (Tai et al., 1997). Second, our animals come from selected lines containing mostly photoperiod responsive or mostly photoperiod nonresponsive mice. Because artificial selection on a single trait (testis size) led to changes in neuronal density, and because photoperiod responsiveness is a heritable, additive genetic trait (Heideman et al., 1999), it is very likely that the differences observed between selected lines are genetic in origin. These genetically distinct lines of mice allow us to test for selected line-specific differences in the photoneuroendocrine

pathway in excitatory or inhibitory photoperiods, whereas many previous experiments on the plasticity of the GnRH neuronal system (Glass 1986; Glass and Knotts, 1987; Korytko et al., 1995; Korytko et al., 1998) required SD conditions in order to unmask photoperiod nonresponsiveness.

The results we obtained using an antibody specific to mature GnRH peptide suggests that differences exist between lines in the neuronal network where mature hormone is synthesized. Significant differences in IR-GnRH cell abundance were found in the preoptic area and anterior hypothalamus (Table 1, Table 5). This suggests that the preoptic and anterior hypothalamic GnRH neurons play a role in seasonal regulation of reproduction and contribute to variation in reproductive responsiveness to photoperiod, while more posterior structures of the hypothalamus are not involved in the mediation of this process. Differences in anterior hypothalamic areas and in preoptic areas approached significance in Experiment 1 (Table 1) and were significant in Experiment 2 (Table 5). A group of ventromedial brain areas did not differ significantly between selected lines in Experiment 1 (Table 1), and a corresponding group of posterior hypothalamic structures did not differ significantly between lines or photoperiods in Experiment 2 (Table 5).

As predicted, animals from a line selected for photoperiod responsiveness had lower overall numbers of IR, mature GnRH-releasing cells than those from a nonresponsive line in SD photoperiod. These results were replicated in Experiment 2, where RM were found to have significantly fewer IR-GnRH cells than NRM in SD and, surprisingly, in LD as well. This suggests that the result obtained for preoptic and anterior hypothalamic structures is a manifestation of the functional importance of this region as one neural site regulating GnRH secretion and SD-induced gonadal regression.

Brain areas that have been implicated as likely sites of action of SD and melatonin on the reproductive axis are variable among mammals (Prendergast et al., 2002), but the AH and MPOA have been implicated previously in *P. leucopus*. Glass and Lynch (1981) and Glass and Knotts (1987) demonstrated that melatonin-containing pellets implanted in the medial POA, AH, and supra- and retrochiasmatic areas, elicit gonadal regression during LD to the same extent as SD exposure. Since melatonin from the pellets was found to diffuse to a distance of only 0.2 mm, and similar doses of melatonin delivered subcutaneously could not trigger testicular regression, it is likely that these neural sites mediate the antigonadal action of melatonin (Glass and Lynch, 1981; Glass and Knotts, 1987).

Glass and Knotts (1987) also showed that melatonin-induced testicular regression during LD is accompanied by changes in the GnRH neuronal system of *P. leucopus*. Melatonin-containing pellets stereotaxically implanted in the AH significantly increased the optical density of IR-GnRH perykarya and the total area covered by IR-GnRH fibers in the ME. The change in intensity and density of the staining was independent of the distance between IR cells and the melatonin implant. Glass and Knotts (1987) used GnRH-BDB for immunocytochemical processing, an antibody reactive to pro-GnRH. The fact that melatonin levels mimicking the effects of SD lead to enhanced immunoreactivity of GnRH perykarya in the AH and medial POA suggests that this treatment increases the intracellular content of the prohormone, and that the antigonadal action of melatonin involves suppression of GnRH release rather than its synthesis (Glass and Knotts, 1987).

Previous experiments by Heideman et al. (1999) demonstrate that the RM and NRM selected lines also differ significantly in their ability to bind melatonin in SD. NRM showed higher 2-[¹²⁵I]iodomelatonin (IMEL) binding in the medial POA and BNST than RM, but no difference was apparent in the dorsomedial nucleus (DMN) of the hypothalamus. This suggests that differences in the density or affinity of the melatonin receptors that ultimately affect mature GnRH secretion are likely to play a role in variability of photoperiod responsiveness (Heideman et al., 1999).

The DMN of the VMH, along with the ventromedial area of the dorsomedial hypothalamus (DMH), constitutes the mediobasal hypothalamus (MBH). The MBH has been identified as the neural site where melatonin mediates seasonal responses to photoperiod in the Syrian hamster (*Mesocricetus auratus*) (Maywood and Hastings, 1995; Maywood et al., 1996). Neurons in the VMH ultimately affect GnRH secreting cells, possibly by responding to gonadal steroids and influencing sensitivity to steroid negative feedback. (Maywood et al., 1996). Lesions to the VMH of male Syrian hamsters have been shown to hasten testicular recrudescence during SD, and it has been suggested that the VMH-DMH complex is critical for the attainment and maintenance of gonadal regression in that species (Bae et al., 1999). Interestingly, we found no differences in IR-GnRH neuron numbers between RM and NRM in these regions in either Experiment 1 or Experiment 2. Relative to our study, this result might be explained with two hypotheses. First, that interneurons expressing melatonin receptors in the VMH help mediate the effects of melatonin on GnRH neurons. Alternatively, it is possible that testicular regression in *P. leucopus* is mediated by the AH and medial POA without input from the

VMH or other posterior hypothalamic nuclei. To our knowledge, there are no published lesion studies of the anterior hypothalamic and preoptic areas of *P. leucopus*.

The differences we observed in IR-GnRH neuron complements between selection lines should be due to differences in responsiveness to photoperiod that are independent of sex-steroid production, as the differences were apparent even when sex-steroid levels were controlled by castration and delivery of a replacement dose of testosterone in Experiment 1. Because all animals in Experiment 1 experienced the same steroid environment prior to immunocytochemical processing, it is unlikely that steroid negative feedback alone is responsible for any differences in the observed numbers of IR-GnRH neurons between RM and NRM. Our method for controlling circulating levels of sex steroids would not, however, account for selected line-specific differences in sensitivity to steroid-negative feedback. Thus, the observed differences in IR-GnRH cell number between RM and NRM in a similar steroid environment might be due to variation in the sensitivity of the reproductive axis to steroid negative feedback.

Our results are consistent with the hypothesis that NRM have higher total numbers of GnRH neurons, which results in a higher number of cells producing mature hormone in NRM than in RM at all times, and permits reproductive activity even if some suppression of GnRH secretion occurs in SD. Thus, variation between selected lines in the number of GnRH neurons producing mature GnRH may have functional significance, and is at least partially responsible for differences in photoperiod responsiveness among *P. leucopus*.

That we were unable to detect differences in the density and location of IR-GnRH cells between photoperiods is remarkable in the context of the differences observed in

paired testis mass and paired seminal vesicle mass of RM and NRM in LD and SD (Table 6; Figure 8), and consistent with at least two hypotheses. First, it is possible that our ICC labeled even minute amounts of mature neuropeptide. Since all GnRH neurons contain at least some mature hormone at any given time, we might have stained nearly the entire neuronal complement in all animals in both SD and LD. However, because we observed IR-neurons of various staining intensities, including some so faint as to be almost undetectable, we suspect that our methods are in fact semi-quantitative in identifying only a subset of the total GnRH neuronal complement. Alternatively, it is possible that mature GnRH synthesis by the GnRH neuronal network does not directly mediate testicular regression and the temporal loss of reproductive capacity in RM under inhibitory photoperiods. Results from Experiment 3 suggest that differential release of mature hormone into the ME, rather than peptide synthesis, might be a key factor mediating gonadal regression in RM.

Our results do not support the hypothesis that genetically based differences in photoperiod responsiveness are accompanied by variation in GnRH fibers, as manifested by differences in the mean fiber content of mature GnRH neuropeptide between selected lines. We did not find statistically significant differences in relative fiber density between selected lines in animals from Experiment 1 or in animals from Experiment 2 at either brain site sampled (Table 6 and Table 7). Within-lines comparisons on the effect of photoperiod on relative fiber density indicate that NRM produce and store roughly the same amount of mature peptide in the GnRH fibers of the preoptic areas in either LD or SD, but release more hormone at the ME under permissive photoperiods (Table 9). RM fibers in the AMPO contain significantly more mature peptide in LD than in SD. RM also

appear to release more mature hormone at the ME under permissive photoperiods (Table 8). This result suggests that some mature GnRH is synthesized and stored in GnRH neurons at all times, but is preferentially released into the ME under permissive photoperiods. Our results indicate that RMLD relative fiber density mean values are higher than NRMLD relative fiber density mean values at both brain sites sampled. This suggests that RM might be able to compensate for their lower total number of GnRH neurons by having each individual neuron synthesize and secrete more hormone (Table 7).

An individual's reproductive status during SD corresponds to its endocrine state. Photoresponsive *P. maniculatus* are known to exhibit lower concentrations of testosterone and LH in SD than in LD, whereas nonphotoresponsive animals in SD maintain circulating levels of both hormones at levels identical to those found during LD (Korytko et al., 1997). In our study, the significantly higher numbers of mature GnRH neurons observed in NRMSD suggest that these individuals are able to secrete a sufficient amount of neuropeptide, even under inhibitory photoperiods, to maintain steady gonadotropin pulsing and release into the bloodstream. The elevated levels of LH and FSH resulting from increased GnRH secretion would, in turn, mediate sufficient testosterone synthesis and spermatogenesis to permit the year-round mating behaviors and fertility that define photoperiod nonresponsiveness (Prendergast et al., 2001).

Total GnRH cell numbers range from 300 to 400 in Djungarian hamsters (Yellon et al., 1990), 650 to 750 in Syrian hamsters (Jennes and Stumpf, 1980), and 500 to 1300 in the rat (Shivers et al., 1993; Wray and Hoffman-Small, 1986). In this study every fourth section was immunocytochemically stained, suggesting that the total number of

IR-GnRH neurons, based on results from Experiment 1, average about 400 in RM and 580 in NRM. Similar total GnRH neuron complements can be projected from our results in Experiment 2, which suggest an average of 400 to 450 cells in RM, and an average of about 700 cells in NRM. These numbers are in the range of the total expected for rodents in this size range, and suggest that a large proportion of total GnRH neurons were immunoreactive in this study.

As previously noted, it is possible that we stained nearly the entire neuronal complement in all animals. If that is the case, then the total reported above accurately estimates the total complement of GnRH neurons in each selected line. If our methods are semi-quantitative, then the total reported above may underestimate the total complement of IR-GnRH neurons in each selected line. The maximum reported diameter of most GnRH neurons is 10 to 20 μm (Silverman et al., 1994), which is consistent with our observation of IR-GnRH perykarya in *P. leucopus*. Our 30- μm coronal sections might have included counts of some cell bodies that were partially within adjacent sections. If so, then the total reported above may slightly overestimate the total complement of IR-GnRH neurons in this population.

Narrow sense heritability (h^2) is the proportion of the total phenotypic variation that is due to the additive effects of genes. This component of variation is relevant because it is the only variation upon which natural selection can act. Previous experiments by Heideman et al. (1999) indicate that photoperiod responsiveness is a heritable, additive genetic trait. One generation of artificial selection on a wild population of *P. leucopus* resulted in a testis index heritability (h^2) mean value of 0.74 ± 0.14 for male offspring on father comparisons. Since testis index and reproductive status are

partially under GnRH control (Silverman et al., 1994; Ebling and Cronin, 2000), and artificial selection for differential testis size in SD resulted in line-specific changes in GnRH neurons, it is likely that the size of the GnRH neuronal complement is heritable as well.

In combination with the results of previous studies on this population (Heideman et al., 1999; Majoy and Heideman, 2000), the presence of variation in this additional trait is consistent with the hypothesis that complex physiological pathways are rarely optimized and that high levels of genetic variation in elements of these pathways may exist within single populations. Results from this study and previous studies of variation within this single population (Heideman et al., 1999; Majoy and Heideman, 2000) are consistent with the adequacy hypothesis. However, more components of this pathway need to be examined in order to obtain an adequate picture of physiological variation.

In summary, mammals can be highly variable within species in life history traits related to reproduction. The photoneuroendocrine pathway studied here is one of the few for which the physiological traits that produce life history variation are being identified systematically and studied within single populations. The implication from the limited data available is that life history variation in this and possibly other pathways is likely to be due to multiple neuroendocrine causes. More studies making these connections are necessary to link variation in life history traits to genes that may contribute to life history variation in natural populations. Closing this gap is important because physiology is the basis of life history evolution, and knowledge of the physiological basis of life history variation is necessary to understand the microevolution of neuroendocrine regulatory pathways.

Chapter 5 – Future Directions:

To answer the question of whether our methods detected nearly all GnRH cells present in the brains of RM and NRM, and to better assess the proportion of cells synthesizing prohormone in SD and LD, we propose a follow-on ICC experiment. This experiment would be carried out on one of the three remaining wells obtained from each perfused brain (see Chapter 2: Materials and Methods, p. 29).

Brains would be processed using a primary antibody known to bind to prohormone only. If it is true that NRM have a larger complement of GnRH neurons, which results in a higher number of cells producing mature hormone in NRM than in RM at all times, we predict that NRM will have a greater number of IR-GnRH cells than RM in any photoperiod. Results from this experiment would also help answer the question of whether GnRH neurons help mediate the loss of reproductive ability observed in RMSD. Based on our results from Experiment 2, we predict that RMLD and RMSD will show no significant differences in the number and distribution of pro-GnRH neurons. We predict that NRMLD and NRMSD will show nearly identical numbers of IR-GnRH perykarya.

The original scope of this work included such an experiment. Two different primary antibodies were used in practice ICC runs: Benoit's pro-GnRH, known to bind to prohormone only; and LR1-GnRH, known to bind both prohormone and mature peptide. Despite multiple attempts with varying antibody concentrations, we were unable to observe any IR-cells. This raises the interesting possibility that *P. leucopus* has a somewhat different GnRH amino acid sequence than the rat (EF Rissman, personal communication). However, since LR1-GnRH is known to be immunoreactive to *P.*

maniculatus GnRH (Korytko et al., 1995; Korytko et al., 1997; Korytko et al., 1998), it is likely that our lack of results is due to problems with our methods.

An experiment to determine how NRM and RM embryos differ in GnRH neuronal complements would help to answer questions regarding the developmental origin of selected line-specific variation in this neuroendocrine pathway. Most GnRH cells emerge from the mitotic cycle and differentiate by E10.5, and commence expressing the prohormone form of GnRH on E11.5 (Wray et al., 1989; Ebling and Cronin, 2000). By E12.5 the number of differentiated cells is similar to the number of cells that make up the adult GnRH complement, suggesting that this population gives rise to all GnRH cells in the adult animal (Silverman et al., 1994). ICC and neuron scoring on embryonic brains ages E10 through E13 would help determine whether NRM GnRH cells begin differentiation earlier in embryonic development than RM cells, stop differentiating later, or differentiate in larger numbers from their neuronal precursor cells.

Until recently, an antagonistic neuropeptide for gonadotropin was unknown. A novel hypothalamic neuropeptide inhibiting gonadotropin release was recently identified in the brain of the Japanese quail *Coturnix japonica* (Tsutsui et al., 2000; Ukena et al., 2003), the song sparrow *Melospiza melodia*, and the house sparrow *Passer domesticus* (Bentley et al., 2003). Gonadotropin inhibitory hormone (GnIH) is a 12 amino acid-long RFa peptide, characterized by the presence of an FMRFamide molluscan neuropeptide-like motif at its C-terminus. GnIH has been shown to significantly inhibit LH release in a dose-dependent manner, but no significant effects on FSH or prolactin release have yet been documented (Tsutsui et al., 2000).

ICC studies have identified clusters of IR-GnIH perykarya in the ventral portion of the PVN of *C. japonica* (Ukena et al., 2003), *M. melodia*, and *P. domesticus* (Bentley et al., 2003). Some scattered IR-cells were observed in the lateral and medial septal areas of *C. japonica*, but not in either species of sparrow. No significant differences in IR-cells could be detected between male and female birds of any of the species sampled (Ukena et al., 2003; Bentley et al., 2003). IR-fibers were widely distributed in the diencephalic and mesencephalic regions of the *C. japonica* brain. Dense IR-fiber networks were seen in the ventral paleostriatum, septal areas, preoptic areas, hypothalamus, and optic tectum. The most prominent IR-fibers projected to the ME and the dorsal motor nucleus of the vagus in the medulla oblongata (Ukena et al., 2003). Double-label ICC and fluorescent ICC studies (Bentley et al., 2003) indicate a high probability of colocalization of GnIH and chicken-GnRH neurons and fibers in the avian brain.

We are unaware of any GnIH ICC or *In situ* hybridization studies on mammals thus far. However, this component of the neuroendocrine pathway appears to have been conserved in rodents, as a working draft sequence for the rat GnIH gene has already been found and is filed in GenBank (Worley, unpublished data). It is possible that GnIH plays a role mediating the process of regression to a prepubertal state that characterizes RM in inhibitory photoperiods, and it represents an additional component for which individual variation in natural populations might exist. Understanding what role GnIH plays in the rodent brain is essential to fully understanding the photoneuroendocrine pathway, and to being able to use it as a model of complex neural systems.

Appendix:

This guide states what structures identified by Eleftheriou and Zolovick in the brain atlas for the deer mouse (1965) correspond spatially to those identified by Paxinos and Watson in the brain atlas for the laboratory rat (1986). It is meant to be an aid for students trying to orient themselves in the preoptic and anterior hypothalamic regions of the *Peromyscus spp.* brain. No claims about functional equivalence are made.

Eleftheriou & Zolovick

Paxinos & Watson

Figure 2

→Plate 9

ACB	Acb & AOP (accumbens nucleus & anterior olfactory nucleus, posterior)
CA	aca (anterior commissure, anterior)
CC	fmi (forceps minor corpus callosum)
CPU	Acb (accumbens nucleus)
FR	RF (rhinal fissure)
MPA	TT (tenia tecta)
OA	No individual structure corresponds
PIR	Pir (piriform cortex) – Corresponds roughly
TOL	lo (lateral olfactory tract)
TUO	TuPO & mfba (olfactory tubercle, polymorph layer & medial forebrain bundle, anterior)

Eleftheriou & Zolovick

Paxinos & Watson

Figure 3

→ **Plate 11** (Figure 3 is intermediate to Plate 10 and Plate 11, but is closer to the latter)

ACB

AcbC (accumbens nucleus, core)

CA

aca (anterior commissure, anterior)

CC

fmi (forceps minor corpus callosum)

CLA

Cl & DEn (claustrum & dorsal endopiriform nucleus)

CPU

CPu (caudate putamen)

DBB

VP & mfba (ventral pallidum & medial forebrain bundle, anterior)

FR

RF (rhinal fissure)

PIR

Pir (piriform cortex) – Corresponds roughly

TOL

lo (lateral olfactory tract)

TP

FStr (fundus striati)

TUO

Tu (olfactory tubercle)

V

LV (lateral ventricle)

Eleftheriou & Zolovick

Paxinos & Watson

Figure 4

→ **Plate 15** (Figure 4 is intermediate to Plate 14 and Plate 15, but is closer to the latter)

ACB	AcbSh & AcbC (accumbens nucleus, shell & accumbens nucleus, core)
CA	aca (anterior commissure, anterior)
CC	cc (corpus callosum)
CLA	Cl & DEn (claustrum & dorsal endopiriform nucleus)
CPU	CPu (caudate putamen)
DBB	VDB & HDB (vertical limb diagonal band & horizontal limb diagonal band)
FR	RF (rhinal fissure)
LS	LSD, LSI, LSV (lateral septal nucleus, dorsal; lateral septal nucleus, intermediate, lateral septal nucleus, ventral)
MFB	mfba (medial forebrain bundle, anterior)
PIR	Pir (piriform cortex) – Corresponds roughly
POA	VP (ventral pallidum)
TOL	lo (lateral olfactory tract)
TP	FStr (fundus striati)
TUO	Tu & VP (olfactory tubercle & ventral pallidum)
V	LV (lateral ventricle)

Eleftheriou & Zolovick

Paxinos & Watson

Figure 5

→ **Plate 16**

AAA	CB (cell bridges ventral striatum)
ACB	Acb (accumbens nucleus)
CA	aca (anterior commissure, anterior)
CC	cc (corpus callosum)
CLA	Cl & DEn (claustrum & dorsal endopiriform nucleus)
CPU	CPu (caudate putamen)
DBB	VDB & HDB (vertical limb diagonal band & horizontal limb diagonal band)
FR	RF (rhinal fissure)
LOT	lo (lateral olfactory tract)
LS	LSD, LSI, LSV (lateral septal nucleus, dorsal; lateral septal nucleus, intermediate, lateral septal nucleus, ventral)
MFB	mfba (medial forebrain bundle, anterior)
MS	MS (medial septal nucleus) – Corresponds roughly
PIR	Pir (piriform cortex) – Corresponds roughly
POA	VP (ventral pallidum)
TUO	Tu (olfactory tubercle) – Corresponds roughly
V	LV (lateral ventricle)

Eleftheriou & Zolovick

Paxinos & Watson

Figure 6

→ **Plate 17** (Figure 6 is intermediate to Plate 17 and Plate 18, but is closer to the former)

AAA

CB (cell bridges ventral striatum)

ACB

FStr & ventral region of CPu (fundus striati & caudate putamen)

BSTMA, BSTL, BSTV (bed nucleus stria terminalis medial division anterior; lateral division; ventral division)

BCA

SHy & VDB (septohypothalamic nucleus & vertical limb diagonal band)

CA

aca (anterior commissure, anterior)

CC

cc (corpus callosum)

CLA

Cl & DEn (claustrum & dorsal endopiriform nucleus)

CPU

CPu (caudate putamen)

FR

RF (rhinal fissure)

LS

LSD, LSI, LSV, PLd (lateral septal nucleus, dorsal; intermediate; ventral; paralambdoid septal nucleus)

MFB

mfa (medial forebrain bundle, anterior)

MS

MS (medial septal nucleus) – Corresponds roughly

PIR

Pir (piriform cortex) – Corresponds roughly

POA

VP (ventral pallidum)

SC

HDB (horizontal limb diagonal band)

TOL

lo (lateral olfactory tract)

V

LV (lateral ventricle)

Eleftheriou & Zolovick

Paxinos & Watson

Figure 7

→ **Plate 20**

AAA	VP & MCPO (ventral pallidum & magnocellular preoptic nucleus)
ACB	FStr & VEn (fundus striati & ventral endopiriform nucleus) BSTMA, BSTL, BSTV (bed nucleus stria terminalis medial division anterior; lateral division; ventral division)
CA	ac & acp (anterior commissure & anterior commissure posterior)
CC	cc (corpus callosum)
CH	SFi (septofimbrial nucleus)
CLA	Cl & DEn (claustrum & dorsal endopiriform nucleus)
CO	ox (optic chiasma)
CPU	CPu (caudate putamen)
FR	RF (rhinal fissure)
FX	f (fornix)
GP	GP, BSTLD, BSTLJ, ic (globus pallidus; bed nucleus stria terminalis lateral division, dorsal; bstld, ventral; internal capsule)
LS	LSD, LSI, LSV, SHy (lateral septal nucleus, dorsal; intermediate; ventral; septohypothalamic nucleus)
MFB	mfba/mfbb, VP (medial forebrain bundle; ventral pallidum)
PIR	Pir (piriform cortex) – Corresponds roughly

POA	LPO, AVPO, MPA (lateral preoptic area, anteroventral preoptic nucleus, medial preoptic area)
SM	st (stria terminalis)
TOL	lo (lateral olfactory tract)
V	LV & 3V (lateral ventricle & 3 rd ventricle)

Eleftheriou & Zolovick

Paxinos & Watson

Figure 8

→ **Plate 22** (Figure 8 is intermediate to Plate 22 and Plate 23, but is closer to the former)

AHA	MPA (medial preoptic area)
AL	VEn (ventral endopiriform nucleus)
ARH	SCh (suprachiasmatic nucleus)
CC	cc (corpus callosum)
CI	ic (internal capsule)
CLA	Cl & DEn (claustrum & dorsal endopiriform nucleus)
CO	ox (optic chiasma)
CPU	CPu (caudate putamen)
FR	RF (rhinal fissure)
FX	f (fornix)
GP	GP (globus pallidus)
LS	LSD & SFi (lateral septal nucleus, dorsal & septofimbrial nucleus)
MFB	AAV, AAD, mfb (anterior amygdaloid area, anterior; dorsal; medial forebrain bundle)
PIR	Pir (piriform cortex) – Corresponds roughly
PT	PT (paratenial thalamus nucleus)
PV	PVA (paraventricular thalamic nucleus, anterior)
PVH	Pe (periventricular hypothalamic nucleus)
SM	sm (stria medullaris thalamus)

ST	st (stria terminalis)
TS	TS & vhc (triangular septal nucleus & ventral hippocampal commissure)
V	LV, 3V, D3V (lateral ventricle; 3 rd ventricle; dorsal 3 rd ventricle)

Eleftheriou & Zolovick

Paxinos & Watson

Figure 9

→ **Plate 24**

ACE	FStr (fundus striati)
AHA	AHA & LA (anterior hypothalamic area, anterior & lateroanterior hypothalamic nucleus)
AL	VE _n (ventral endopiriform nucleus)
AM	AM (anteromedial thalamic nucleus)
AME	LOT 2, 3 (nucleus lateral olfactory tract)
ARH	SCh (suprachiasmatic nucleus)
AV	AVDM & AVVL (anteroventral thalamic nucleus, dorsomedial & anteroventral thalamic nucleus, ventrolateral)
CC	cc (corpus callosum)
CI	ic (internal capsule)
CLA	Cl & DEn (claustrum & dorsal endopiriform nucleus)
CO	ox (optic chiasma)
CPU	CPu (caudate putamen)
FR	RF (rhinal fissure)
FX	f (fornix)
GP	GP (globus pallidus)
LS & TS	fi & TS (fimbria hippocampus & triangular septal nucleus)
MFB	SI & SM (substantia innominata & nucleus stria medullaris)

PIR	Pir (piriform cortex) – Corresponds roughly
PT	PT (paratenial thalamus nucleus)
PV	PVA (paraventricular thalamic nucleus, anterior)
PVH	PaAP (paraventricular hypothalamic nucleus, anterior)
RE	Re & VRe (reuniens thalamic nucleus & ventral reuniens nucleus)
RT	Rt (rhomboid thalamic nucleus)
SM	sm (stria medullaris thalamus)
SO	SO & HDB (supraoptic nucleus & nucleus horizontal limb diagonal band)
ST	st (stria terminalis)
V	LV, 3V, D3V (lateral ventricle; 3 rd ventricle; dorsal 3 rd ventricle)
ZI	Rt on plate 24; ZI (zona incerta) on plate 25

Eleftheriou & Zolovick

Paxinos & Watson

Figure 10

→Plate 25

ACE	AStr & CeL (amygdalostriatal transition area & central amygdaloid nucleus, lateral)
ACO	ACo (anterior cortical amygdaloid nucleus)
AD	AD (anterodorsal thalamic nucleus)
AHA	AHC (anterior hypothalamic area, central)
AL	BLA & I (basolateral amygdaloid nucleus, anterior & intercalated nuclei amygdala)
AM	AM & IAM (anteromedial thalamic nucleus & interanterodorsal thalamic nucleus)
AME	MeA (medial amygdaloid nucleus, anterior)
ARH	Pe (periventricular hypothalamic nucleus)
AV	AVDM & AVVL (anteroventral thalamic nucleus, dorsomedial & anteroventral thalamic nucleus, ventrolateral)
CC	cc (corpus callosum)
CH & FX	CA3, DG, dhc, fi (field CA3 of Ammon's horn; dentate gyrus; dorsal hippocampal commissure; fimbria hippocampus)
CI	ic (internal capsule)
CLA	DEn (dorsal endopiriform nucleus)
CPU	CPu (caudate putamen)
FR	RF (rhinal fissure)
FX	f (fornix)
GP	GP (globus pallidus)

LHA	TC (tuber cinereum)
LM	VM (ventromedial thalamic nucleus)
MD	CM (central medial thalamic nucleus)
MFB	LH/mfb & MCPO (lateral hypothalamic area/medial forebrain nucleus & magnocellular preoptic nucleus)
MT	mt (mammillothalamic tract)
OT	opt & sox (optic tract & supraoptic decussation)
PIR	Pir (piriform cortex) – Corresponds roughly
PT	PT (paratenial thalamus nucleus)
PV	PVA (paraventricular thalamic nucleus, anterior)
RE	Re & VRe (reuniens thalamic nucleus & ventral reuniens nucleus)
RT	Rt (rhomboid thalamic nucleus)
SM	sm/MHb (stria medullaris thalamus/medial habenular nucleus)
ST	st (stria terminalis)
V	LV, 3V, D3V (lateral ventricle; 3 rd ventricle; dorsal 3 rd ventricle)
VA	VL (ventrolateral thalamic nucleus)
ZI	Rt on plate 24; ZI (zona incerta) on plate 25

Eleftheriou & Zolovick

Paxinos & Watson

Figure 11

→**Plate 26** (Figure 11 is intermediate to Plate 26 and Plate 27, but is closer to the former)

ABL	BLA & IM (basolateral amygdaloid nucleus, anterior & intercalated amygdaloid nucleus, main)
ACE	AStr, CeLCn, CeLC (amygdalostriatal transition area; central amygdaloid nucleus, lateral division central; central amygdaloid area, lateral division capsular)
ACO	ACo (anterior cortical amygdaloid nucleus)
AD	AD (anterodorsal thalamic nucleus)
AHA	AHP (anterior hypothalamic area, posterior)
AL	LaDL (lateral amygdaloid nucleus, dorsolateral)
AM	AM & IAM (anteromedial thalamic nucleus & interanterodorsal thalamic nucleus)
AME	MeAD & MeAV (medial amygdaloid nucleus, anterodorsal & medial amygdaloid nucleus, anteroventral)
ARH	Arc (arcuate hypothalamic nucleus)
AV	AV (anteroventral thalamic nucleus)
CC	cc (corpus callosum)
CH & FI	CA3, DG, dhc, fi (field CA3 of Ammon's horn; dentate gyrus; dorsal hippocampal commissure; fimbria hippocampus)
CI	ic (internal capsule)
CLA	DEn (dorsal endopiriform nucleus)
CPU	CPu (caudate putamen)

FR	RF (rhinal fissure)
FX	f (fornix)
GP	GP (globus pallidus)
HPC	DHC & part of CA3 (nucleus dorsal hippocampal commissure & field CA3 of Ammon's horn)
LHA	LH & TC (lateral hypothalamic area & tuber cinereum)
LT	LDVL (laterodorsal thalamic nucleus, ventrolateral)
MD	CM (central medial thalamic nucleus)
MFB	LH/mfb & MCPO (lateral hypothalamic area/medial forebrain bundle & magnocellular preoptic nucleus)
MT	mt (mammillothalamic tract)
OT	opt & sox (optic tract & supraoptic decussation)
PT	MD & MDL (mediodorsal thalamic nucleus & mediodorsal thalamic nucleus, lateral)
PV	PVA (paraventricular thalamic nucleus, anterior)
PVH	VM (ventromedial thalamic nucleus)
RE	Re & VRe (reuniens thalamic nucleus & ventral reuniens nucleus)
RH	Rh & G (rhomboid thalamic nucleus & gelatinosus thalamic nucleus)
SM	sm, MHb, LHb (stria medullaris thalamus; medial habenular nucleus; lateral habenular nucleus)

ST	st (stria terminalis)
V	LV, 3V, D3V (lateral ventricle; 3 rd ventricle; dorsal 3 rd ventricle)
VA & VE	VL & VPL (ventrolateral thalamic nucleus & ventral posterolateral thalamic nucleus)
ZI	ZI (zona incerta)

Eleftheriou & Zolovick

Paxinos & Watson

Figure 12

→Plate 28

ABL	BLA & BMA (basolateral amygdaloid nucleus, anterior & basomedial amygdaloid nucleus, anterior)
ACE	BSTIA, CeLCn, CeLC (bed nucleus stria terminalis, intraamygdala division; central amygdaloid nucleus, lateral division central; central amygdaloid area, lateral division capsular)
ACO	ACo (anterior cortical amygdaloid nucleus)
AL	La (lateral amygdaloid nucleus)
AM	CM & PC (central medial thalamic nucleus & paracentral thalamic nucleus)
AME	Me & MePV (medial amygdaloid nucleus & medial amygdaloid nucleus, posteroventral)
AV	Ang & Po (angular thalamic nucleus & posterior thalamus nuclear group)
CC	cc (corpus callosum)
FI	fi (fimbria hippocampus)
CI	ic (internal capsule)
CLA	DEn & VEn (dorsal endopiriform nucleus & ventral endopiriform nucleus)
CPU	CPu (caudate putamen)
DMH	DMD (dorsomedial hypothalamic nucleus, diffuse)
FD	DG (dentate gyrus)
FR	RF (rhinal fissure)

FX	f (fornix)
HM & HL	LHb & MHb (lateral habenular nucleus & medial habenular nucleus)
HPC	CA1 & CA2 (field CA1 & field CA2 of Ammon's horn)
LHA	LH & TC (lateral hypothalamic area & tuber cinereum)
LM	Border region of ZI & VM (zona incerta & ventromedial thalamic nucleus)
LT	LDVL & LDDM (laterodorsal thalamic nucleus, ventrolateral & laterodorsal thalamic nucleus, dorsomedial)
MD	IMD, MDM, MDPL (intermediodorsal thalamic nucleus; mediodorsal thalamus nucleus, medial; mediodorsal thalamic nucleus, paralamina)
MFB	LH/mfb (lateral hypothalamic area/medial forebrain bundle)
MT	mt (mammillothalamic tract)
OT	opt & sox (optic tract & supraoptic decussation)
PIR	Pir (piriform cortex)
PT	MDC & MDL (mediodorsal thalamic nucleus, central & mediodorsal thalamic nucleus, lateral)
PV	PV (paraventricular thalamic nucleus)
PVH	DA (dorsal hypothalamic area)
RE	Re & VRe (reuniens thalamic nucleus & ventral reuniens nucleus)
RH	Rh & G (rhomboid thalamic nucleus & gelatinosus thalamic nucleus)

RT	Rt (reticular thalamic nucleus)
SM	sm (stria medullaris)
ST	st & cst (stria terminalis & commissural stria terminalis)
V	LV, 3V, D3V (lateral ventricle; 3 rd ventricle; dorsal 3 rd ventricle)
VA & VE	VL, VPM, VPL (ventrolateral thalamic nucleus; ventral posterolateral thalamic nucleus; ventral posterolateral thalamic nucleus)
ZI	ZI (zona incerta)

Eleftheriou & Zolovick

Paxinos & Watson

Figure 13

→Plate 30

ABL	BLA & BM (basolateral amygdaloid nucleus, anterior & basomedial amygdaloid nucleus)
ACE	BSTIA & CeL (bed nucleus stria terminalis, intraamygdala division & central amygdaloid nucleus, lateral)
ACO	PMCo & PLCo (posteromedial cortical amygdala nucleus)
AL	LaDL, LaVL, BLP (lateral amygdaloid nucleus, dorsolateral; lateral amygdaloid nucleus, ventrolateral; basolateral amygdaloid nucleus, posterior)
AME	MePD & MePV (medial amygdaloid nucleus, posterodorsal & medial amygdaloid nucleus, posteroventral)
CC	cc (corpus callosum)
FI	CA2 & CA3 ((field CA2 & field CA3 of Ammon's horn)
CI	ic (internal capsule)
CL	SubI (subincertal nucleus)
CLA	DEn & VEn (dorsal endopiriform nucleus & ventral endopiriform nucleus)
CPU	CPu (caudate putamen)
DMH	DM (dorsomedial hypothalamic nucleus)
FD	DG & PoDG (dentate gyrus & polymorph layer dentate gyrus)
FR	RF (rhinal fissure)

FX	f (fornix)
HM & HL	LHb & MHb (lateral habenular nucleus & medial habenular nucleus)
HPC	CA1 & CA2 (CA1 and CA2 fields of Ammon's horn)
LHA	MTu (medial tuberal nucleus)
LM	eml (external medullary lamina)
LT	LDVL & LDDM (laterodorsal thalamic nucleus, ventrolateral & laterodorsal thalamic nucleus, dorsomedial)
MD	IMD, MDC, MDL, CL (intermediodorsal thalamic nucleus; mediodorsal thalamus nucleus, central; mediodorsal thalamic nucleus, lateral; centrolateral thalamic nucleus)
MFB	LH/mfb (lateral hypothalamic area/medial forebrain bundle)
MT	mt (mammillothalamic tract)
OT	opt & sox (optic tract & supraoptic decussation)
PIR	Pir (piriform cortex)
PT	MDM (mediodorsal thalamic nucleus, medial)
PV	PVP (paraventricular thalamic nucleus, posterior)
RE	Re & VRe (reuniens thalamic nucleus & ventral reuniens nucleus)
RH	Rh & G (rhomboid thalamic nucleus & gelatinosus thalamic nucleus)
RT	Rt (reticular thalamic nucleus)

SM	sm (stria medullaris)
ST	st (stria terminalis)
V	LV, 3V, D3V (lateral ventricle; 3 rd ventricle; dorsal 3 rd ventricle)
VD & VE	VPL, VPM (ventral posterolateral thalamic nucleus; ventral posteromedial thalamic nucleus)
VM	VM (ventromedial thalamic nucleus)
ZI	ZI (zona incerta)

Eleftheriou & Zolovick *Peromyscus sp.* Atlas Abbreviations

A: Aqueductus cerebri (Sylvius)

AAA: Area amygdaloidea anterior

ABL: Nucleus amygdaloideus basalis pars lateralis

ACB: Nucleus accumbens septi (Area parolfactoria lateralis)

ACE: Nucleus amygdaloideus centralis

ACO: Nucleus amygdaloideus corticalis

AD: Nucleus anterodorsalis thalami

AHA: Area anterior hypothalami

AL: Nucleus amygdaloideus lateralis

AM: Nucleus anteromedialis thalami

AME: Nucleus amygdaloideus medialis

ARH: Nucleus arcuatus hypothalami

AV: Nucleus anteroventralis thalami

BCA: Nucleus proprius commissurae anterioris (Bed nucleus)

BCS: Brachium colliculi superioris

CA: Commissura anterior

CC: Corpus callosum

CH: Commissura hippocampi (Commissura fornicis)

CI: Capsula interna

CIF: Colliculus inferior

CL: Nucleus subthalamicus (Luys)

CLA: Claustrum

CO: Chiasma opticum

CP: Commissura posterior

CPU: Nucleus caudatus / Putamen

CS: Colliculus superior

CSC: Commissura colliculi superioris

CT: Nucleus centralis tegmenti (Bechterew)

D: Nucleus Darkschewitz

DBB: Gyrus diagonalis (Diagonal band of Broca)

DBC: Decussatio brachiorum coniunctorum

DMH: Nucleus dorsomedialis hypothalami

DTD: Decussatio tegmenti dorsalis (Meynert)

DTV: Decussatio tegmenti ventralis (Forel)

FA: Fissura amygdaloidea

FD: Gyrus dentatus (Fascia dentata)

FH: Fissura hippocampi

FI: Fimbria hippocampi

FLD : Fasciculus longitudinalis dorsalis (Schutz)

FLM : Fasciculus longitudinalis medialis

FR : Fissura rhinalis

FX: Fornix (Corpus, columna)

GL: Corpus geniculatum laterale

GM: Corpus geniculatum mediale

GP: Globus pallidus

HL: Nucleus habenularis lateralis

HM: Nucleus habenularis medialis

HP: Tractus habenulo-interpeduncularis (Fasciculus retroflexus)(Meynert)

HPC: Hippocampus (Cornu Ammonis)

IP: Nucleus interpeduncularis

LHA: Area lateralis hypothalami

LM: Lemniscus medialis

LS: Nucleus lateralis septi

LT: Nucleus lateralis thalami

LTP: Nucleus lateralis thalami pars posterior

MD: Nucleus mediodorsalis thalami

MFB: Fasciculus medialis telencephali (Medial forebrain bundle)

ML: Nucleus mamillaris lateralis

MM: Nucleus mamillaris medialis

MP: Nucleus mamillaris posterior

MPA: Area parolfactoria medialis

MS: Nucleus medialis septi

MT : Tractus mamillo-thalamicus (Vicq d'Azyr)

NCP: Nucleus proprius commissurae posterioris (Bed nucleus)

NPT: Nucleus posterior thalami

NR: Nucleus ruber

OA: Nucleus olfactorius anterior

OT: Tractus opticus

P: Pons

PC: Pedunculus cerebri

PF: Nucleus parafascicularis thalami

PH: Nucleus posterior hypothalami

PIR: Cortex piriformis

PMD: Nucleus premamillaris dorsalis

PMV: Nucleus premamillaris ventralis

POA: Area preoptica (medialis, lateralis)

PRT: Area pretectalis

PT: Nucleus parataenialis thalami

PV: Nucleus paraventricularis thalami

PVH: Nucleus paraventricularis hypothalami

RE: Nucleus reuniens thalami

RF: Formatio reticularis (mesencephali)

RH: Nucleus rhomboideus thalami

RT: Nucleus reticularis thalami

SC: Nucleus suprachiasmaticus

SM: Stria medullaris thalami

SN: Substantia nigra

SO: Nucleus supraopticus hypothalami

ST: Stria terminalis (Tasnia semicircularis)

SUM: Area supramamillaris

TS: Nucleus triangularis septi

TT: Tractus mamillo-tegmentalis

TUO: Tuberculum olfactorium

V: Ventriculus cerebri

VA: Nucleus ventralis thalami pars anterior

VD: Nucleus ventralis thalami pars dorsomedialis

VE: Nucleus ventralis thalami

VM: Nucleus ventralis thalami pars medialis

VMH: Nucleus ventromedialis hypothalami

ZI: Zona incerta

II: Nervus opticus

III: Nervus oculomotorius; Nucleus nervi oculomotorii

V: Nucleus tractus mesencephalici nervi trigemini

Bibliography:

- MM Aarts and M Tymianski, Molecular mechanisms underlying specificity of excitotoxic signaling in neurons. *Curr Mol Med* 4(2) (2004) 137-47.
- JP Adelman, AJ Mason, JS Hayflick and PH Seeburg, Isolation of the gene and hypothalamic cDNA for the common precursor of gonadotropic-releasing hormone and prolactin release-inhibiting factor in human and rat. *Proc Natl Acad Sci* 83 (1986) 179-183.
- RS Ahima, D Prabakaran, C Mantzoros, D Qu , B Lowell, E Maratos-Flier and JS Flier, Role of leptin in the neuroendocrine response to fasting. *Nature* 382 (1996) 250–252.
- HH Bae, RA Mangles, BS Cho, J Dark, SM Yellon and I Zucker, Ventromedial hypothalamic mediation of photoperiodic gonadal responses in male Syrian hamsters. *J Biol Rhythms* 14(5) (1999) 391-401.
- GA Bartholomew, Interspecific comparison as a tool for ecological physiologists. In: ME Feder, AF Bennet, WW Burggren and RB Huey (Eds.), *New Directions in Ecological Physiology*, Cambridge University Press, Cambridge, 1987, pp. 11-35.
- TJ Bartness, JB Powers, H Hastings, EL Bittman and BD Goldman, The times infusion paradigm for melatonin delivery: What has it taught us about the melatonin signal, its reception, and the photoperiodic control of seasonal responses?. *J Pineal Res* 15 (1993) 161-190.
- GE Bentley, N Perfito, K Ukena, K Tsutsui and JC Wingfield, Gonadotropin-inhibitory peptide in song sparrows (*Melospiza melodia*) in different reproductive conditions, and in house sparrow (*Passer domesticus*) relative to chicken-gonadotropin-releasing hormone. *J Neuroendocrinol* 15 (2003) 794-802.
- LM Besecke and JE Levine, Acute increases in responsiveness of luteinizing hormone (LH)-releasing hormone nerve terminals to neuropeptide-Y stimulation before the preovulatory LH surge. *Endocrinology* 135 (1994) 63–66.
- GD Bittner and BX Friedman, Evolution of brain structures and adaptive behaviors in humans and other animals: role of polymorphic genetic variations. *Neuroscientist* 6(4) (2000) 241-251.
- MS Boyce MS, Evolution of life histories: Theory and patterns from mammals. In: MS Boyce (Ed.), *Evolution of Life Histories of Mammals*, Yale University Press, Chelsea, 1988, pp. 3-30.

- FH Bronson, The regulation of luteinizing hormone secretion by estrogen: Relationships among negative feedback, surge potential, and male stimulation in juvenile, peripubertal, and adult female mice. *Endocrinology* 108 (1981) 506-516.
- FH Bronson, *Mammalian Reproductive Biology*. The University of Chicago Press, Chicago, 1989. pp 48-53.
- FH Bronson and PD Heideman, Seasonal regulation of reproduction in mammals. In: E Knobil and JD Neill (Eds.), *The Physiology of Reproduction*, Second ed., Raven Press, New York, 1994, pp. 541-584.
- C Catzeflis, DD Pierroz, F Rohner-Jeanrenaud, JE Rivier, PC Sizonenko and ML Aubert, Neuropeptide Y administered chronically into the lateral ventricle profoundly inhibits both the gonadotropic and the somatotrophic axis in intact adult female rats. *Endocrinology* 132 (1993) 224–234.
- WP Chen, JW Witkin and AJ Silverman, Sexual dimorphism in the synaptic input to gonadotropin releasing hormone neurons. *Endocrinology* 126 (1990) 695–702.
- MA Cowley, JL Smart, M Rubinstein, MG Cerdan, S Diano, TL Horvath, RD Cone and MJ Low, Leptin activates anorexigenic POMC neurons through a neural network in the arcuate nucleus. *Nature* 411 (2001) 480–484.
- WF Crowley and SP Kalra, Neuropeptide Y stimulates the release of luteinizing hormone-releasing hormone from medial basal hypothalamus in vitro: Modulation by ovarian hormones. *Neuroendocrinology* 46 (1987) 97–103.
- FC Davis, Melatonin: Role in development. *J Biol Rhythms* 12(6) (1997) 498-508.
- RA DeFazio, S Heger, SR Ojeda and SM Moenter, Activation of GABA_A receptors excites gonadotropin-releasing hormone neurons. *Mol Endocrinol* 16 (2002) 2872–2891.
- FJP Ebling and AS Cronin, The neurobiology of reproductive development. *Neuroreport* 11(16) (2000) R23-R32.
- BE Eleftheriou and AJ Zolovick, *The Forebrain of the Deermouse in Stereotaxic Coordinates*. Kansas State University, Technical Bulletin 146 (1965).
- DL Foster, FJ Ebling, AF Micka, LA Vannerson, DC Bucholtz, RI Wood, JM Suttie and DE Fenner, Metabolic interfaces between growth and reproduction: Nutritional modulation of gonadotropin, prolactin, and growth hormone secretion in the growth-limited female lamb. *Endocrinology* 125 (1989) 342–350.

- ME Freeman, The neuroendocrine control of the ovarian cycle of the rat. In: E Knobil and JD Neill (Eds.), *The Physiology of Reproduction*, Second ed., Raven Press, New York, 1994, pp 613-658.
- T Garland Jr., Selection experiments: An underutilized tool in biomechanics and organismal biology. In: VL Bels, JP Gasc, A Casinos (Eds.), *Biomechanics and Evolution*. Oxford, Bios Scientific Publishers, 2002.
- JD Glass and GR Lynch, Melatonin: Identification of sites of antigonadal action in mouse brain. *Science* 214 (1981) 821-823.
- JD Glass, Short photoperiod-induced gonadal regression: Effects of gonadotropin-releasing hormone (GnRH) neuronal system of the white-footed mouse, *Peromyscus leucopus*. *Biol Reprod* 35 (1986) 733-743.
- JD Glass and LK Knotts, A brain site for the antigonadal action of melatonin in the white-footed mouse (*Peromyscus leucopus*): Involvement of the immunoreactive GnRH neuronal system. *Neuroendocrinology* 46 (1987) 48-55.
- BD Goldman, Mammalian photoperiodic system: Formal properties and neuroendocrine mechanisms of photoperiodic time measurement. *J Biol Rhythms* 16 (2001) 283-301.
- DG Hazlerigg, What is the role of melatonin within the anterior pituitary?. *J Endocrinol* 170(3) (2001) 493-501.
- PD Heideman and FH Bronson, Characteristics of a genetic polymorphism for reproductive photoresponsiveness in the white-footed mouse (*Peromyscus leucopus*). *Biol Reprod* 44(6) (1991) 1189-1196.
- PD Heideman, TA Bruno, JW Singley and JV Smedley, Genetic variation in photoperiodism in *Peromyscus leucopus*: Geographic variation in an alternative life-history strategy. *J Mammal* 80(4) (1999) 1232-1242.
- PD Heideman, SL Kane and AL Goodnight, Differences in hypothalamic 2-[¹²⁵I]iodomelatonin binding in photoresponsive and non-photoresponsive white-footed mice, *Peromyscus leucopus*. *Brain Res* 840 (1999) 56-64.
- PD Heideman, Top-down approaches to the study of natural variation in complex physiological pathways using the white-footed mouse (*Peromyscus leucopus*) as a model. *ILAR* 45(1) (2004) 4-13.
- S Hosny and L Jennes, Identification of the α_{1B} Adrenergic Receptor Protein in Gonadotropin Releasing Hormone Neurones of the Female Rat. *J Neuroendocrinol* 10(9) (1998) 687-692.

- HT Jansen, C Cutter, S Hardy, MN Lehman and RL Goodman, Seasonal plasticity within the GnRH system of the ewe: Changes in identified GnRH inputs and in glial association. *Endocrinology* 144 (2003) 3663–3676.
- L Jenness and WE Stumpf, LHRH-systems in the brain of the golden hamster. *Cell Tissue Res* 290 (1980) 239-256.
- JD Johnston, S Messenger, FJP Ebling, LM Williams, P Barrett and DG Hazlerigg, Gonadotrophin-releasing hormone drives melatonin receptor down-regulation in the developing pituitary gland. *Proc Natl Acad Sci* 100(5) (2003) 2831–2835.
- SP Kalra and PS Kalra, Neural regulation of luteinizing hormone secretion in the rat. *Endocrine Reviews* 4(4) (1983) 311-350.
- SP Kalra, MG Dube, A Sahu, CP Phelps and PS Kalra, Neuropeptide Y secretion increases in the paraventricular nucleus in association with increased appetite for food. *Proc Natl Acad Sci* 88 (1991) 10931–10935.
- LW Kao and J Weisz, Release of gonadotrophin-releasing hormone (Gn-RH) from isolated, perfused medial-basal hypothalamus by melatonin. *Endocrinology* 100(6) (1977) 1723-1726.
- LJ Kriegsfeld, R Silver, AC Gore and D Crews, Vasoactive Intestinal Polypeptide Contacts on Gonadotropin-Releasing Hormone Neurons Increase Following Puberty in Female Rats. *J Neuroendocrinol* 14 (2002) 685–690.
- AI Korytko, J Marcelino and JL Blank, Differential testicular responses to short daylength in deer mice are reflected in the GnRH neuronal system. *Brain Res* 685 (1995) 135-142.
- AI Korytko, DE Dluzen and JL Blank, Photoperiod and steroid-dependent adjustments in hypothalamic gonadotropic hormone-releasing hormone, dopamine, and norepinephrine content in male deer mice. *Biol Reprod* 56 (1997) 617-624.
- AI Korytko, SH Vessey and JL Blank, Phenotypic differences in the GnRH neuronal system of deer mice *Peromyscus maniculatus* under a natural short photoperiod. *J Reprod Fertil* 114 (1998) 231-235.
- SL Lindstedt and JH Jones, Symmorphosis: The concept of optimal design. In: ME Feder, AF Bennet, WW Burggren and RB Huey (Eds.), *New Directions in Ecological Physiology*, Cambridge University Press, Cambridge, 1987, pp. 289-309.
- SL Lindstedt and SD Swain, Body size as a constraint of design and function. In: MS Boyce (Ed.), *Evolution of Life Histories of Mammals*, Yale University Press, Chelsea, 1988, pp. 93-105.

- GR Lynch and SL Gendler, Multiple responses to different photoperiods occur in the mouse, *Peromyscus leucopus*. *Oecologia* 45 (1980) 318-321.
- SB Majoy and PD Heideman, Tau differences between short-day responsive and short-day nonresponsive white-footed mice (*Peromyscus leucopus*) do not affect reproductive photoresponsiveness. *J Biol Rhythms* 15(6) (2000) 501-513.
- JE Martin and C Sattler, Developmental loss of the acute inhibitory effect of melatonin on the *in vitro* pituitary luteinizing hormone and follicle-stimulating hormone responses to luteinizing hormone-releasing hormone. *Endocrinology* 105(4) (1979) 1007-1012.
- ES Maywood and MH Hastings, Lesions of the iodomelatonin-binding sites of the mediobasal hypothalamus spare the lactotropic, but block the gonadotropic response of male Syrian hamsters to short photoperiod and to melatonin. *Endocrinology* 136(1) (1995) 144-153.
- ES Maywood, EL Bittman and MH Hastings, Lesions of the melatonin- and androgen-responsive tissue of the dorsomedial nucleus of the hypothalamus block the gonadal response of male Syrian hamsters to programmed infusions of melatonin. *Biol Reprod* 54 (1996) 470-477.
- JM Meredith, FW Turek and JE Levine, Pulsatile luteinizing hormone responses to intermittent N-methyl-D,L-aspartate administration in hamsters exposed to long- and short-day photoperiods. *Endocrinology* 129(4) (1991) 1714-1720.
- RB Norgren Jr. and R Brackenbury, Cell adhesion molecules and the migration of LHRH neurons during development. *Dev Biol.* 160(2) (1993) 377-87.
- ML Ovesjo, M Gamstedt, M Collin and B Meister, GABAergic nature of hypothalamic leptin target neurons in the ventromedial arcuate nucleus. *J Neuroendocrinol* 13 (2001) 505-516.
- G Paxinos and C Watson, *The rat brain in stereotaxic coordinates*. Academic Press, San Diego, CA, 1986.
- BJ Prendergast, LJ Kriegsfeld and RJ Nelson, Photoperiodic polyphenisms in rodents: Neuroendocrine mechanisms, costs, and functions. *Quart Rev Biol* 76 (2001) 293-325.
- BJ Prendergast, B Mosinger Jr., PE Kolattukudy and RJ Nelson, Hypothalamic gene expression in reproductively photoresponsive and photorefractory Siberian hamsters. *Proc Natl Acad Sci* 99(25) (2002) 16291-16296.
- BJ Prendergast, RJ Nelson and I Zucker, Mammalian seasonal rhythms: Behavioral and neuroendocrine substrates. In: DW Pfaff, A Arnold, A Etgen, S Fahrbach and R

Rubin (Eds.), *Hormones, Brain, and Behavior*, Academic Press, New York, 2002, pp. 93-156.

- N Pronchuk, AG Beck-Sickinger and WF Colmers WF, Multiple NPY receptors inhibit GABA_A synaptic responses of rat medial parvocellular effector neurons in the hypothalamic paraventricular nucleus. *Endocrinology* 143 (2002) 535–543.
- S Pu, MR Jain, TL Horvath, S Diano, SP Kalra and SP Kalra, Interactions between neuropeptide Y and gamma-aminobutyric acid in stimulation of feeding: A morphological and pharmacological analysis. *Endocrinology* 140 (1999) 933–940.
- PD Raposinho, DD Pierroz, P Broqua, RB White, T Pedrazzini and ML Aubert, Chronic administration of neuropeptide Y into the lateral ventricle of C57BL/6J male mice produces an obesity syndrome including hyperphagia, hyperleptinemia, insulin resistance, and hypogonadism. *Mol Cell Endocrinol* 185 (2001) 195–204.
- D Roy and DD Belsham, Melatonin receptor activation regulates GnRH gene expression and secretion in GT1-7 GnRH neurons. *Signal transduction mechanisms. J Biol Chem* 277(1) (2002) 251-258.
- JR Sauer and NA Slade, Body size as a demographic categorical variable: Ramifications for life history analysis of mammals. In: MS Boyce (Ed.), *Evolution of Life Histories of Mammals*, Yale University Press, Chelsea, 1988, pp. 107-121.
- M Schwanzel-Fukuda, GR Reinhard, S Abraham, KL Crossin, GM Edelman and DW Pfaff, Antibody to neural cell adhesion molecule can disrupt the migration of luteinizing hormone-releasing hormone neurons into the mouse brain. *J Comp Neurol* 342(2) (1994) 174-185.
- BD Shivers, RE Harlan, JI Morrell and DW Pfaff, Immunocytochemical localization of luteinizing hormone-releasing hormone in male and female rat brains. *Neuroendocrinology* 36 (1983) 1-12.
- AJ Silverman, EA Zimmerman, MJ Gibson, MJ Perlow, HM Charlton, GJ Kokoris and DT Krieger, Implantation of normal fetal preoptic area into hypogonadal mutant mice: Temporal relationships of the growth of gonadotropin-releasing hormone neurons and the development of the pituitary/testicular axis. *Neuroscience* 16 (1985) 69–84.
- AJ Silverman, GJ Kokoris and MJ Gibson, Quantitative analysis of synaptic input to gonadotropin-releasing hormone neurons in normal mice and hpg mice with preoptic area grafts. *Brain Res* 443 (1988) 367–372.
- AJ Silverman, I Livne and JW Witkin, The gonadotropin-releasing hormone (GnRH), neuronal systems: Immunocytochemistry and in situ hybridization. In: E. Knobil

and J.D. Neill (Eds.), *The Physiology of Reproduction*, Second ed., Raven Press, New York, 1994, pp 1683-1709.

- JA Sim, MJ Skynner, JR Pape and AE Herbison, Late postnatal reorganization of GABA_A receptor signalling in native GnRH neurons. *Eur J Neurosci* 12 (2000) 3497–3504
- PF Smith and JD Neill, Simultaneous measurement of hormone release and secretagogue binding by individual pituitary cells. *Proc Natl Acad Sci* 84 (1987) 5501-5505.
- SC Stearns, The influence of size and phylogeny on patterns of covariation among life-history traits in the mammals. *Oikos* 41 (1983) 173-187.
- SD Sullivan and SM Moenter, γ -Aminobutyric acid neurons integrate and rapidly transmit permissive and inhibitory metabolic cues to gonadotropin-releasing hormone neurons. *Endocrinology* 145(3) (2004) 1194-1202.
- SD Sullivan, RA Defazio and SM Moenter, Metabolic regulation of fertility through presynaptic and postsynaptic signaling to gonadotropin-releasing hormone neurons. *J Neurosci* 23 (2003) 8578–8585.
- SD Sullivan, LC Howard, AH Clayton and SM Moenter, Serotonergic activation rescues reproductive function in fasted mice: Does serotonin mediate the metabolic effects of leptin on reproduction?. *Biol Reprod* 66 (2002) 1702–1706.
- VC Tai, PA Schiml, X Li and EF Rissman, Behavioral interactions have rapid effects on immunoreactivity of prohormone and gonadotropin-releasing hormone peptide. *Brain Res* 772 (1997) 87-94.
- E Terasawa, Control of luteinizing hormone-releasing hormone pulse generation in nonhuman primates. *Cell Mol Neurobiol* 15(1) (1995) 141-164.
- K Tsutsui, E Saigoh, K Ukena, H Teranishi, Y Fujisawa, M Kikuchi, S Ishii and PJ Sharp, A novel avian hypothalamic peptide inhibiting gonadotropin release. *Biochemical and Biophysical Research Communications* 275 (2000) 661-667.
- K Ukena, T Ubuka and K Tsutsui, Distribution of a novel avian gonadotropin-inhibitory hormone in the quail brain. *Cell Tissue Res* 312 (2003) 73-79.
- EM van der Beek, VM Wiegant, HA van der Donk, R van den Hurk and RM Buijs, Lesions of the suprachiasmatic nucleus indicate the presence of a direct vasoactive intestinal polypeptide-containing projection to gonadotrophin-releasing hormone neurons in the female rat. *J Neuroendocrinol* 5(2) (1993) 137–144.
- EM van der Beek, HJ van Oudheusden, RM Buijs, HA van der Donk, R van den Hurk and VM Wiegant, Preferential induction of c-fos immunoreactivity in vasoactive

intestinal polypeptide-innervated gonadotropin-releasing hormone neurons during a steroid-induced luteinizing hormone surge in the female rat. *Endocrinology* 134 (1994) 2636-2644.

EM van der Beek, VM Wiegant, HJ van Oudheusden, HA van der Donk, R van den Hurk and RM Buijs, Synaptic contacts between gonadotropin-releasing hormone-containing fibers and neurons in the suprachiasmatic nucleus and perichiasmatic area: An anatomical substrate for feedback regulation?. *Brain Research* 755 (1997) 101-111.

J Vanecek, Melatonin binding sites. *Neuroendocrinology* 48 (1988) 201-203.

DR Weaver, LL Carlson and SM Reppert, Melatonin receptors and signal transduction in melatonin-sensitive and melatonin-insensitive populations of white-footed mice (*Peromyscus leucopus*). *Brain Res* 506(2) (1990) 353-357.

ER Weibel, CR Taylor and L Bolis, Principles of Animal Design: The Optimization and Symmorphosis Debate. Cambridge University Press, New York, 1998.

SR Wersinger, DJ Haisenleder, DB Lubahn and EF Rissman, Steroid feedback on gonadotropin release and pituitary gonadotropin subunit mRNA in mice lacking a functional estrogen receptor alpha. *Endocrine* 11(2) (1999) 137-43.

MJ Will, EB Franzblau and AE Kelley, Nucleus accumbens μ -opioids regulate intake of a high-fat diet via activation of a distributed brain network. *J Neurosci* 23 (2003) 2882-2888.

JW Witkin, Synaptology of luteinizing hormone-releasing hormone neurons in the preoptic area of the male rat: Effects of gonadectomy. *Neuroscience* 29 (1989) 385-390.

PA Witt-Enderby, J Bennett, MJ Jarzynka, S Firestine, MA Melan, Melatonin receptors and their regulation: Biochemical and structural mechanisms. *Life Sci* 72(20) (2003) 2183-2198.

S Wray and GE Hoffman-Small, Postnatal morphological changes in rat LHRH neurons correlated with sexual maturation. *Neuroendocrinology* 43 (1986) 93-97.

SM Yellon and SW Newman, A developmental study of the gonadotropin-releasing hormone neuronal system during sexual maturation in the male djungarian hamster. *Biol Reprod* 45 (1991) 440-446.

SM Yellon, SW Newman and MN Lehman, The gonadotropin releasing hormone neuronal system of the male djungarian hamster: Distribution from the olfactory tubercle to the medial basal hypothalamus. *Neuroendocrinology* 51 (1990) 219-225.

Vita:

Mauricio Avigdor Villanueva

Mauricio Avigdor was born in the city of Lima, Perú on October 10, 1977. He graduated from Liceo Moral y Luces Herzl-Bialik in Caracas, Venezuela on July 26 of 1995. Mauricio Avigdor received his B.S. at The College of William and Mary in 1999 with a degree in Biology. Mr. Avigdor taught High School Biology and Environmental Sciences during the 1999-2000 school year. In January of 2001 he entered the graduate program in Biology at The College of William and Mary in Williamsburg, Virginia and began work towards the degree of Master of Arts in Biology from that institution.